

# IOWA STATE UNIVERSITY

## Digital Repository

---

Graduate Theses and Dissertations

Iowa State University Capstones, Theses and  
Dissertations

---

2013

## Influence of conductive network composite thickness and structure on performance of ionic polymer-metal composite transducer

Wangyujue Hong  
*Iowa State University*

Follow this and additional works at: <https://lib.dr.iastate.edu/etd>



Part of the [Mechanical Engineering Commons](#)

---

### Recommended Citation

Hong, Wangyujue, "Influence of conductive network composite thickness and structure on performance of ionic polymer-metal composite transducer" (2013). *Graduate Theses and Dissertations*. 13109.  
<https://lib.dr.iastate.edu/etd/13109>

This Thesis is brought to you for free and open access by the Iowa State University Capstones, Theses and Dissertations at Iowa State University Digital Repository. It has been accepted for inclusion in Graduate Theses and Dissertations by an authorized administrator of Iowa State University Digital Repository. For more information, please contact [digirep@iastate.edu](mailto:digirep@iastate.edu).



[www.manaraa.com](http://www.manaraa.com)

**Influence of conductive network composite thickness and structure on performance  
of ionic polymer-metal composite transducer**

by

**Wangyujue Hong**

A thesis submitted to the graduate faculty

In partial fulfillment of the requirements for the degree

MASTER OF SCEINCE

Major: Mechanical Engineering

Program of Study Committee:

Reza Montazami, Major Professor

Michael Kessler

Xinwei Wang

Iowa State University

Ames, Iowa

2013

Copyright © Wangyujue Hong, 2013. All rights reserved.

## TABLE OF CONTENT

LIST OF TABLES .....	iv
LIST OF FIGURES .....	v
CHAPTER 1 Background and Literature Review .....	1
1.1 Introduction .....	1
1.2 Ionomeric membrane in IPMC transducer .....	3
1.3 Ionic liquids in IPMC transducer .....	5
1.4 Conductive network composite in IPMC transducer .....	7
1.4.1 Introduction.....	7
1.4.2 CNC layers prepared by impregnation-reduction process .....	8
1.4.3 CNC layers prepared by direct assembly process.....	9
1.4.4 CNC layers prepared by layer by layer self-assembly process.....	10
1.5 Summary .....	13
Reference.....	14
CHAPTER 2 Influence of Conductive Network Composite Thickness on Electromechanical and Mechanoelectrical Performance of Ionic Polymer-Metal Composite Transducer .....	19
Abstract .....	19
2.1 Introduction .....	20
2.2 Experimental section .....	24
2.2.1 The fabrication of IPMC transducer .....	24
2.2.2 Characterization of samples.....	25
2.3 Results and discussion.....	27
2.3.1 Characterization of CNC layers in IPMC .....	27
2.3.2 Characterization of actuation performance in IPMC .....	32
2.3.3 Characterization of sensing performance in IPMC.....	34
2.4 Conclusion.....	37
Reference.....	39
CHAPTER 3 Ionic Effect of Sodium Chloride on the Conductive Network Composite Nanostructure and its Influence on the Performance of Ionic Polymer-Metal Composite Transducers .....	41
Abstract .....	41

3.1 Introduction .....	42
3.2 Experimental section .....	44
3.3 Results and discussion.....	45
3.3.1 Ionic strength effect on CNC layer formation .....	45
3.3.2 Ionic strength effect on actuation performance in IPMC.....	49
3.3.3 Ionic strength effect on sensing performance in IPMC .....	50
3.4 Conclusion.....	52
Reference.....	55
 CHAPTER 4 Future Prospective .....	57
4.1 Exploration of cytotoxicity of IPMC transducer.....	57
4.2 Exploration of effect of nanoparticles size and shape on IPMC transducer performance .....	62
Reference.....	66
 Acknowledgement .....	67

**LIST OF TABLES**

Table 2.1 Thickness of different components of variety of transducers. ....	26
Table 3.1 Intercepts and slopes of the fitted lines of cationic and anionic curvatures.....	49

## LIST OF FIGURES

Fig. 1.1 Chemical composition of Nafion.....	4
Fig. 1.2 Cluster-network model for Nafion membranes proposed by Gierke et.al.....	5
Fig. 1.3 Chemical structure of 1-ethyl-3-methylimidazolium trifluoromethanesulfonate ionic liquid.....	7
Fig. 1.4 Schematic representation of ionic polymer metal composite prepared by reduction method .....	9
Fig. 1.5 Schematic of the film deposition process using slide and beakers. Beakers with polycation and polyanion represent the adsorption process; beakers with water represent washing step. The order of polycation and polyanion depends on the original surface charge of the slide. In this schematic, we assume the slide has negative surface charge before LbL deposition. ....	11
Fig. 2.1 Schematic representation of an IPMC transducer; as actuator, the IPMC will bend under an electrical signal; as sensor, the IPMC will generate an electrical signal in response to mechanical stress.....	21
Fig. 2.2 Schematic representation of the transducer structure with CNC layers via LBL self-assembly deposition.....	24
Fig. 2.3 SEM image of 20 bilayers of AuNPs/PAH on Nafion.....	25
Fig. 2.4 Schematic representation of the sample to be tested for quasi-static and dynamic sensing response.....	27
Fig. 2.5 (a) UV-Vis absorbance spectrum of growing process of AuNPs/PAH thin-film. (b) Digital microscopy images for different number of bilayers of AuNPs/PAH (left to right 10, 20, 30 and 40 bilayers). .....	28
Fig. 2.6 Sheet resistance decreases significantly as the number of AuNPs/PAH bilayers increased.....	29
Fig. 2.7 Electrical impedance of IPMC actuators with different number of bilayers comprising the CNC. ....	30
Fig. 2.8 Photographic images of an IPMC-based actuator with 30 bilayers of AuNPs/PAH in CNC; electrode on the right side is anode. ....	33
Fig. 2.9 (a) Net cationic and anionic strains, and (b) cationic and anionic actuation curvatures increase linearly with the increase in the number of bilayers in CNC....	34
Fig. 2.10 IPMC based sensor covered between two electrical tapes with Cu as electrode for bending deformation. Top line are lateral views before and after bending; bottom line are corresponding top views. ....	36
Fig. 2.11 IPMC sensor response in the form of output voltage when IPMC sensor is subject to a bending deformation. Left is the output voltage from sample 1 and the right is the output voltage from sample 2. ....	36
Fig. 2.12 IPMC sensor response in the form of output voltage when IPMC sensor is subject to a dynamic vibration impact by a motor. Black line represents the output voltage from sample 1 and red line represents the output voltage from sample 2....	37
Fig. 3.1 Schematic representation of the effects of salt concentration in the solvent environment on the conformation of polyelectrolyte; (a) low ionic strength (low salt concentration); (b) high ionic strength (high salt concentration). ....	43
Fig. 3.2 UV-Vis absorbance spectra of (a) AuNPs solution (20ppm); (b) growing process of AuNPs/PAH thin-film with different salt concentrations in PAH solution.	

The lines from the bottom up in each color represent 2, 4, 6, 8, 10 bilayers of AuNPs/PAH thin-film respectively .....	45
Fig. 3.3 Difference of sheet resistance between group 1 and 2. For both groups, sheet resistance decreases significantly as the number of AuNPs/PAH bilayers increased. ....	47
Fig. 3.4 Cationic and anionic bending curvatures (Q) of group 1 and 2; for each group, Q increases linearly with the increased number of bilayers. Both cationic and anionic curvatures in group 2 are higher than those in group 1.....	49
Fig. 3.5 IPMC sensor response in the form of output voltage when IPMC sensor is subject to a bending deformation. From left to right is the voltage generated by the sample with bare Nafion membrane (0 bilayer), 40 bilayers from group 1 and 40 bilayers from group 2.....	51
Fig. 3.6 IPMC sensor response in the form of output voltage when IPMC sensor is subject to a dynamic vibration impact by a motor. Black line is corresponding to the sample with bare Nafion membrane (0 bilayer), red and blue lines are corresponding to the samples with 40 bilayers from group 1 and 2 respectively. ....	52
Fig. 4.1 Formation of AuNPs/PAH thin-film via LbL process. ....	58
Fig. 4.2 Formation of CuNPs/PSS thin-film via LbL Process. ....	58
Fig. 4.3 Cyclic voltammograms of (a) bare ITO coated glass, (b) PAH/PSS thin-film, (c) AuNPs/PAH thin-film, and (d) CuNPs/PSS thin-film taken at 10-100 mV/s scan rates (10 mV/s increments). Inset in (c) and (d) : peak current vs. square root of scan rate indicates diffusion controlled process.....	59
Fig. 4.4 Cyclic voltammograms of AuNPs/PAH thin-film taken at 10-100 mV/s scan rates (10 mV/s increments). Black lines represent CV result of thin-film with no NaCl in PAH solution while the red lines represent CV result of thin-film with 200 mM NaCl in PAH solution. Arrow indicates increasing scan rate. ....	61
Fig. 4.5 Synthesis process of AuNRs via seed mediated method. ....	63
Fig. 4.6 (a) UV-Vis absorbance spectra of AuNRs with different Ag ion concentrations; (b) TEM image of AuNRs with aspect ratio around 2.3. ....	64
Fig. 4.7 UV-Vis absorbance spectra of growing process of AuNRs/PSS multilayer film. ....	64

## CHAPTER 1

### Background and Literature Review

#### 1.1 Introduction

In the last two decades, more and more attention has been paid to understand operation mechanism, and to improve the performance of mechano-electric transducers[1, 2]. Interesting applications for such transducers are presented in different fields, including bio-mimetic devices, biomedical devices, microrobotics and microfluidics[1, 3-7]. In these applications, smart polymers have attracted significant attention due to their low cost, low density, ease of processing and high sensitivity to stimulus[8]. Because of these unique properties, ionic electroactive polymers (IEAPs), a new class of smart structure based on mobility of ions within the polymeric network, plays a more and more important role in the application of electromechanical and mechanoelectrical devices.

IEAPs belong to a class of smart structures that exhibit mechano-electric behavior. The mechanical response is due to the transport of different size ions caused by an external electrical stimulus, and their accumulation at the oppositely-charged electrodes; which, will lead to a volume imbalance between the two sides of the structure and thus mechanical deformation of the structure[9]. Moreover, it has been proved that the electromechanical phenomenon is reversible for many IEAP devices, meaning they respond to an applied mechanical force by generating an electrical signal. The sensing principle is due to the mobility of free ions which results in generating of an electrical field across the thickness of the structure, that is collected by the IEAP device structure[10]. Among the IEAP devices, ionic polymer-metal composite (IPMC) is one of the most extensively studied class during the last several years due to a number of

promising characteristics and their potential applications in the areas such as soft robotic actuators, artificial muscles and dynamic sensors.

To the best of the author's knowledge, the very first report of the ionic chemomechanical deformation comes from Kuhn *et.al*[11-13]. They found a three-dimensional network containing polyelectrolytes such as polyacrylic acid (PAA) or polyvinyl chloride (PVA) system, if suspended in water, can contract and dilate reversibly upon alternating addition of small amounts of acid and alkali to the medium[11]. They also pointed out that the shape of ionizable polymeric molecules depends on the number of charges distributed over the molecular chain[13]. Besides, a co-polymer, PVA-PAA has been proved to be a typical system which also has dimension changes depending on their chemical environment by Hamlen *et.al* in 1965[14]. They also proved that the same deformation can be obtained electrically since the applied voltage causes the solution to become either acidic or alkaline depending on the direction of the current. Later, the present of an electrically controlled mechanical deformation model comes from Grodzinsky *et.al* at the first time at 1973[15, 16]. They studied and developed collagen and other polyelectrolyte-based materials in an electrochemical environment as the seat of a mechanical response resulting from an electrical stimulus and an electrical response to a mechanical deformation. Moreover, a model presenting the membrane at the inter-fibrillar level was developed relating externally measured parameters and membrane intrinsic properties[16].

More recently related interest in this area can be traced to Shahinpoor and his co-workers. In their earlier works (before 1996), Shahinpoor *et.al* focused more on the study of ionic polymeric gels for the robotic applications. As talked before, ionic polymeric

gels, better known as artificial muscles, are three-dimensional networks of cross-linked macromolecular polymers that can change their initial volume in a liquid medium based on the addition of acid or alkali. As early as 1992, Shahinpoor *et.al* have discussed a structure design, kinematics and swimming dynamics of autonomous swimming robotic structures based on the electrically controlled ionic polymeric gels[17]. After that they published a series of experimental studies focused on the ionic polymeric gels for robotic applications and presented corresponding theoretical models for exact expressions and further study[18–21].

Subsequently Mojarrad and Shahinpoor gave rise to a new composite of ion exchange membranes (IEM) and platinum through chemically treating with platinum salt solution as electrically controllable artificial muscles firstly in 1996[22]. This work provides a platform for their further studies of IPMC for biomimetic sensors, actuators and artificial muscles. More complete and interesting work can be found in the following references[23–25] and they also did a series of four review papers focusing on fundamentals, manufacturing techniques, modeling and simulation, and industrial and medical application of ionic polymer –metal composites[1, 5–7].

## **1.2 Ionomeric membrane in IPMC transducer**

IPMC materials are made of a thin ionomer membrane with typical thickness no larger than 100  $\mu\text{m}$ [6]. Nafion® (DuPont) is one of the most common used ion-exchange membranes, and its chemical structure is shown in Fig. 1.1, where the value of m can be as low as 1 and n varies from 5 to 11. The value of x in the following structure represents the degree of sulfonation of the polymer, and it determines the equivalent weight (EW) of the membrane, which is defined as the weight of dry polymer per mole of exchange sites.

Typically, for Nafion the value of x ranges between 6 and 14 and its corresponding EW is from 1000 to 1800. Fig. 1.1 shows the form of Nafion after hydrolyzed and the sulfonate exchange sites at the ends of side chains can be linked with proton and some other cations such as  $\text{Na}^+$ ,  $\text{K}^+$  and  $\text{Li}^+$ .

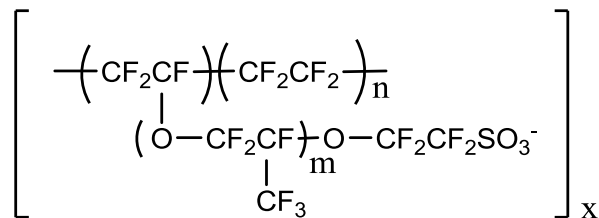


**Fig. 1.1 Chemical composition of Nafion.**

Considering the unique chemical structure of ionomers, some different models have been proposed for the interpretation of their morphology, such as (i) two-phase model proposed by Cooper *et.al* [26]and (ii) Core-shell model proposed by Macknight, Stein and their coworkers[27]. Nafion membrane has a Teflon-like backbone with different side chains. The sulfonate exchange sites at the ends of these side chains are strongly hydrophilic while the backbone of the polymer is strongly hydrophobic. Moreover, the specific location of the exchange sites makes them less fixed so as to position themselves in their preferred orientation to some extent. Based on the two models of ionomers proposed before and these unique chemical structures of Nafion talked before, a so-called cluster network model first proposed by Gierke *et.al* at 1982 becomes the most generally accepted theory to describe the specific morphology of Nafion polymer[17, 18]. They presented that the sulfonate exchange sites and counter-ions of the polymer reside on the inner surface of ionic cluster phase while the hydrophobic backbone portion of the polymer forms the inert fluorocarbon matrix outside of the cluster phase. In this model, the ionic clustering is believed to be an approximately spherical, inverted micellar

structure and interconnected each other by short, narrow channels. The hydrophilic phase separates into approximately spherical domains, and the ionic exchange sites are found near the interface between two phases. This model satisfies the tendency for the sulfonic acid sites to be hydrated very well, and at the same time, it decreases the opportunity of the unfavorable interaction between water and the hydrophobic fluorocarbon matrix. Fig. 1.2 is a schematic representation of the cluster network model for Nafion perfluorinated membrane, and the dimensions of the clusters (diameter and separation distance) were deduced from experiments[29]. This unique chemical structure provides Nafion a specific transport property from other ionic polymers and promotes its applications in many fields especially in the area of IPMC sensors and actuators.

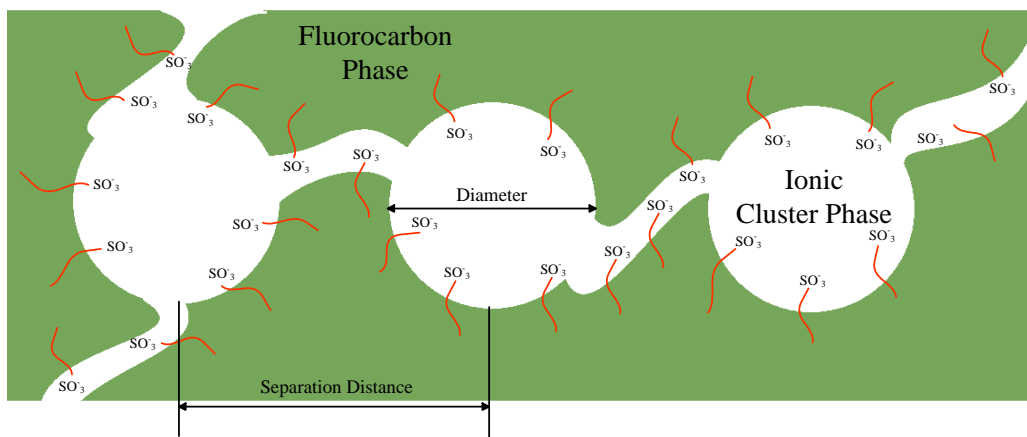


**Fig. 1.2 Cluster-network model for Nafion membranes proposed by Gierke et.al.**

### 1.3 Ionic liquids in IPMC transducer

Two thin layers of noble metal electrodes such as platinum and gold are coated on the two sides of the ionomer membrane. Due to the fixed anions on the backbone of polymer membrane, same amount freely movable cations (typically  $\text{Na}^+$ ,  $\text{K}^+$ ,  $\text{Li}^+$  and  $\text{Cs}^+$  in water solution) also exist in the membrane[10]. It is the redistribution of these movable

cations that cause the actuation and sensing in the materials when the material is saturated with a solvent. Typically, the solvent is water based, but there are some limitations for the IPMC materials in an aqueous solution. First water is easily to evaporate in air and it affects the mobility of cations significantly in the IPMC matrix. Also, when they are applied in actuation, external electrical stimulus will be imposed on the IPMC materials, which, however, will induce the decomposition of water into hydrogen and oxygen through electrolysis. Therefore, finding another solvent which can facilitate transduction in the IPMC materials but reduce or eliminate the two problems caused by aqueous solution seems to be more and more necessary. Nemat-Nasser and Zamani have adopted ethylene glycol as solvent for IPMC materials to eliminate the evaporation and electrolysis problems associated with water[30]. They also found when compared with the IPMC materials with water as solvent, the IPMCs with ethylene glycol as solvent have greater solvent uptake. However, the actuation-speed will decrease significantly so they can only be applied when high-speed actuation is not necessary. Also, Shahinpoor and Kim have demonstrated a new solid-state polymer actuators made with poly(ethylene oxide) and poly(ethylene glycol) (PEO-PEG)[31]. In this case, PEO promised an ionic conductivity within itself due to the existence of an amorphous region in the material, while PEG is known to decrease the crystallinity of the host medium and increase the ion mobility by improving miscibility with the amorphous region. In the other word, PEO-PEG serves as polar host matrices for salts to facilitate motion of the cations.

In recent years, a new compound, ionic liquids (ILs) have been investigated as possible new electrolyte for IPMC materials due to their high voltages stability and very low vapor pressure when compared with water-solvent polyelectrolytes[32]. Ionic liquid

is a salt in the liquid state at or below room temperature. The ionic bound is usually stronger than Van der Waals force, which is between the molecules of ordinary liquids. That is why common salts trend to be solid and cannot melt to liquid state until very high temperature, such as NaCl, whose melting temperature is around 800 °C. However, room temperature ionic liquids consist of bulky and asymmetric organic cations and a wide range of anions from organic to inorganic. The bulky and cumbersome structure of the corresponding ions will inhibit the formation of a crystalline solid, which is the main reason that they tend to be liquid state at or below room temperature. Some published works have proved that ionic liquid 1-ethyl-3-methylimidazolium trifluoromethanesulfonate (EMI-Tf) can provide a better attribution to the IPMC materials application in actuation[33, 34]. The structure of this ionic liquid is shown in Fig. 1.3.

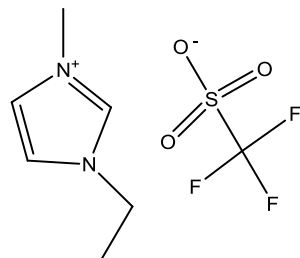


**Fig. 1.3 Chemical structure of 1-ethyl-3-methylimidazolium trifluoromethanesulfonate ionic liquid.**

## 1.4 Conductive network composite in IPMC transducer

### 1.4.1 Introduction

Experimental results indicated that a higher population of excess charges at the electrodes is preferred for both actuating and sensing properties. Therefore, porous electrodes which can provide higher contact areas between electrodes and ionic polymers have been adopted during the transducer design and fabrication process. Usually, two

conductive network composite (CNC) layers are deposited between the two sides of the ionic polymer layer to improve the porosity of electrodes and act as reservoirs for electrolyte. It has been proved that most electrical and mechanical properties of the CNC layers such as conductivity, volume density, porosity and pore size have a direct effect on the IPMC properties[35]. The improvement of the porous electrodes offers larger electrode areas in contact with ionomer membrane, so that a higher population of the excess charges can be accumulated at the electrodes, which, is beneficial for a higher electromechanical and mechanoelctrical signals generation by the ionic polymer transducers[36, 37]. Also, a relative thicker CNC layer can reserve a larger population of movable cations in electrolyte among the transducers based on IPMC materials and improve their actuation and sensing performance significantly[38]. Based on the advantages mentioned above, a number of researches have been focused on the control of the properties of CNC layers.

#### **1.4.2 CNC layers prepared by impregnation-reduction process**

A widely used method at earlier study is plating metal cation complex onto the ionomer membrane surface at first, and then nanosized metal particles would be obtained by chemical reduction method for penetrating into the ionomer membrane. In this way, the interfacial area between the polymer and the metal is very large, which is beneficial for the formation of porous electrodes and a larger capacitance of these devices[39]. The adsorption-reduction method process is represented in Fig. 1.4. Millet and Andolfatto *et.al* proposed a model for the chemical reduction of platinum tetramine and Nafion film and utilized this model to study the rate of ion-exchange[40] and investigate the precipitation process[41]. Rashid and Shahinpoor[42] also utilized the

similar reduction process for the study of ionic polymeric platinum composite artificial muscles. Onishi and Sewa *et.al* [36] adopted the sequential adsorption/reduction cycling to grow a suitable pair of gold electrodes with a fractal-like structure to improve a higher interfacial area between the electrodes and polymer electrolytes so that led to a larger electromechanical deformation.

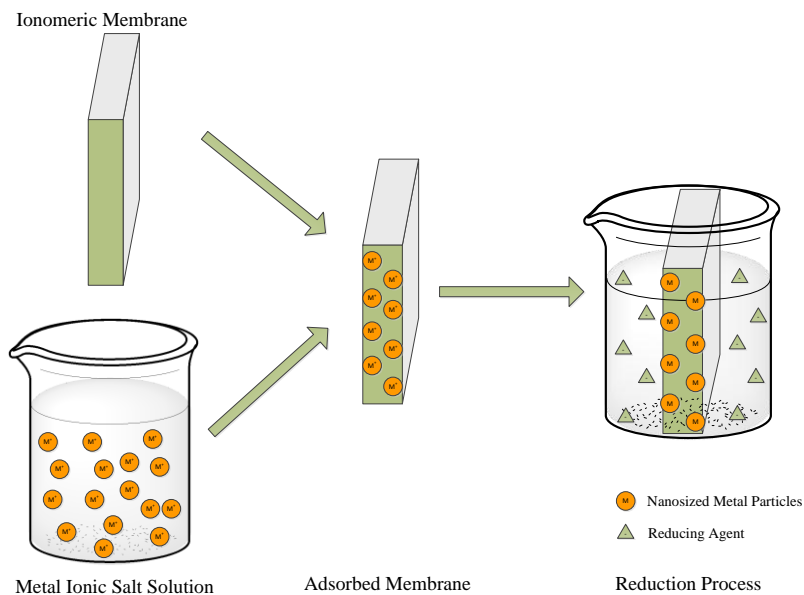


**Fig. 1.4 Schematic representation of ionic polymer metal composite prepared by reduction method**

#### 1.4.3 CNC layers prepared by direct assembly process

Although the impregnation-reduction process is a reliable method, it still has some limitations in the critical parameters control, such as the control over electrode morphology and composition. To eliminate these drawbacks, a novel method on the manipulating of electroding process, direct assembly process (DAP), has been proposed by Akle and Leo[8, 43-45]. They mixed an ionic polymer solution with conductor nanoparticles and deposited the mixture on the Nafion (or other ionomer) membrane as an electrode. This method increases the effective interfacial area then the capacitance

(between five and ten times higher than that obtained using a standard impregnation-reduction process) of electrodes observably. Also, the performance of the transducers has been proved to exceed the performance of the original one by a factor of between 2 and 5[43]. The novel direct assembly method is attractive because it provides a large range of the use of conductive nanosized powder in the fabrication of IPMCs, which is no longer limited in metals but can be extended to some other materials including carbon nanotubes[44].

#### **1.4.4 CNC layers prepared by layer by layer self-assembly process**

Layer-by-layer (LbL) self-assembly technique has been studied for several decades because they are flexible and allow the access and implementation of nanoscale structure and order, which has led to a number of advances in materials science. Although carbon-based molecules offer an enormous structure diversity and various potential application ranging from optics, electronics, aerospace, biological and mechanical engineering, they also suffer from some problems such as sensitive to heat or light, easy to be oxidized, low intensity and dehydration. The ability to fine tune multicomposites with an easy controlled structure on the nano- or microscale becomes necessary for combining two or more desirable properties and avoiding their weakness at the same time. As early in 1980s, self-assembly techniques have been proposed for assembling of artificial layered structures based on covalent monolayer-surface binding (chemisorption) and intralayer cross-linking[46]. However, consider the restrictions of covalent chemisorption including the high demanding of steric structure and reaction environment, certain classes of organics utilization and high-quality films still cannot be satisfied. To yield nanoarchitecture film with good positioning of individual layers and easy controlled

fabrication process, a novel technique, LbL self-assembly adsorption from aqueous solution was proposed by Decher group at early 1990s[47-50].

To be shortly, LbL self-assembly deposition, is a nanofabrication technique based on use of oppositely charged polyelectrolytes, DNA, conducting polymers, proteins, and metal or semiconductor nanoparticles. LbL self-assembly deposition is a fast, simple, inexpensive method for fabrication of thin-films which allows nanoscale control over the structure. In this technique, the substrate is alternately exposed to cationic and anionic species. Each exposure forms one layer and charge of each layer is the foundation to the next layer. One whole cycle consists of exposure to cationic solution, rinsing, exposure to ionic solution, and rinsing, which forms one bilayer. Fig. 1.5 represents a schematic of the LbL deposition process using slide and beakers.

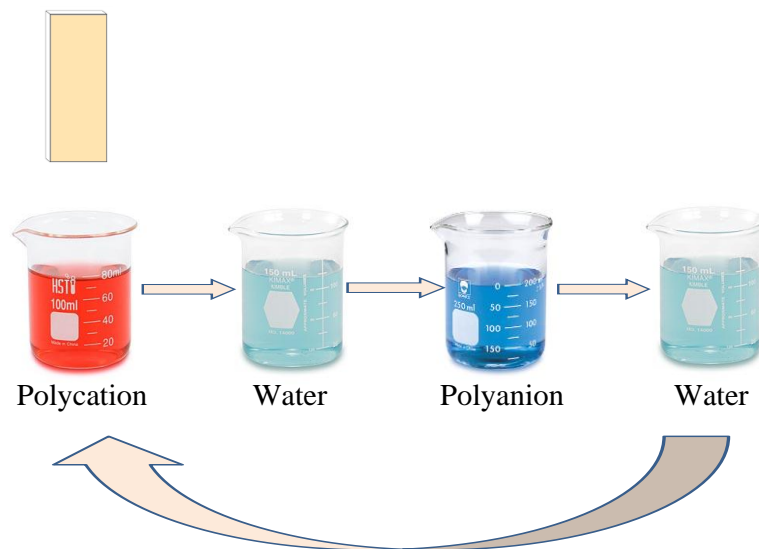


**Fig. 1.5 Schematic of the film deposition process using slide and beakers. Beakers with polycation and polyanion represent the adsorption process; beakers with water represent washing step. The order of polycation and polyanion depends on the original surface charge of the slide. In this schematic, we assume the slide has negative surface charge before LbL deposition.**

Electrostatically LbL assembly technique offers freedom in materials selection and structural design, which gives many advantages in comparison with other methods. One

major advantage of LbL self-assembly technique is that the different kinds of active elements can be incorporated into thin-films without significant alteration of their electrical and chemical properties. It is possible to make a blending at the nano-meter scale, and various components in these thin-films can be tuned on a molecular level, which is beneficial to enhance electron and ion transport and energy transfer within the layers[51]. Also, many attractive features have been promoted for the thin-film attained by this method. First, the multilayers formed by LbL deposition is uniform and free of defect, thus it guarantees the elimination of the failure led by impurities, surface defects or crystalline defects. Also, the thickness control of thin-film is accurate to tens of nanometers, and the conductance of such films is one or two orders of magnitude higher in comparison to the films made by other methods such as spin-cast and screen-coating. Moreover, the thin-film can be deposited onto rich variety of substrates, including conductive surface such as ITO coated glass or film, flexible surface such as ionomeric membrane (Teflon or Nafion), and even colloidal substrates. Based on the unique performance of LbL technique, more recent studies have expended on the use of these thin-films as the basis of devices in variable areas including perm-selective thin-film[52-57], electrochromic thin-films[58-61], nanomechanical thin-films[62, 63], biomedical implant devices and therapeutic delivery[64, 65].

More recently, another attractive application of LbL self-assembly technique was investigated by Montazami and Liu *et.al* about a new class of CNC layers in the manufacture of ionic polymer conductor network composite(IPCNC) actuators[9, 33, 34, 36, 38]. Experimental results indicated that a better electromechanical behavior of IPMC actuators can be achieved by adopting the gold nanoparticles (AuNPs) and polycation

poly(allylamine hydrochloride) (PAH) to form a porous CNC layers. The CNC layers added to the ionomer membrane were to act as reservoirs for electrolyte and improve the performance of interface. LbL technique was employed to construct the porous structure and keep the CNC layers thickness in the nanometer range[47, 51]. They have proposed a corresponding model for this electrode structure[34, 66] and proved that both the thickness[38] and the structure[9] of the CNC layers have an obvious effect on the actuation performance.

### 1.5 Summary

This work is focused on the actuation and sensing behaviors of IPMC transducers with Nafion as ionomer membrane, ionic liquid EMI-Tf as electrolyte, and AuNPs/PAH thin-film via LbL self-assembly as CNC layers. The hypothesis of this work is that the thickness and structure of CNC layers will play an important role on determining the performance of IPMC transducers. We verify this hypothesis through a series of thoughtful works and the corresponding experimental results and discussion will be represented in the next chapters.

## Reference

- [1] M. Shahinpoor and K. J. Kim, “Ionic polymer–metal composites: IV. Industrial and medical applications,” *Smart Materials and Structures*, vol. 14, no. 1, pp. 197–214, Feb. 2005.
- [2] C. Bonomo, P. Brunetto, L. Fortuna, P. Giannone, S. Graziani, and S. Strazzeri, “A Tactile Sensor for Biomedical Applications Based on IPMCs,” *IEEE Sensors Journal*, vol. 8, no. 8, pp. 1486–1493, Aug. 2008.
- [3] E. Mbemmo, Z. Chen, S. Shatara, and X. Tan, “Modeling of Biomimetic Robotic Fish Propelled by an Ionic Polymer-Metal Composite Actuator,” *Robotics and Automation, IEEE International Conference*, pp. 689–694, 2008.
- [4] B. Kim, D.-H. Kim, J. Jung, and J.-O. Park, “A biomimetic undulatory tadpole robot using ionic polymer–metal composite actuators,” *Smart Materials and Structures*, vol. 14, no. 6, pp. 1579–1585, Dec. 2005.
- [5] M. Shahinpoor and K. Kim, “Ionic polymer-metal composites: I. Fundamentals,” *Smart Materials and Structures*, vol. 10, no. 4, pp. 819–833, 2001.
- [6] K. J. Kim and M. Shahinpoor, “Ionic polymer metal composites: II. Manufacturing techniques,” *Smart Materials and Structures*, vol. 12, no. 1, pp. 65–79, Feb. 2003.
- [7] M. Shahinpoor and K. J. Kim, “Ionic polymer–metal composites: III. Modeling and simulation as biomimetic sensors, actuators, transducers, and artificial muscles,” *Smart Materials and Structures*, vol. 13, no. 6, pp. 1362–1388, Dec. 2004.
- [8] B. J. Akle, M. D. Bennett, and D. J. Leo, “High-strain ionomer–ionic liquid electroactive actuators,” *Sensors and Actuators A: Physical*, vol. 126, no. 1, pp. 173–181, Jan. 2006.
- [9] R. Montazami, D. Wang, and J. Heflin, “Influence of conductive network composite structure on the electromechanical performance of ionic electroactive polymer actuators,” *International Journal of Smart and Nano Materials*, vol. 3, no. 3, pp. 204–213, 2012.
- [10] D. Pugal, K. Jung, A. Aabloo, and K. J. Kim, “Ionic polymer-metal composite mechanoelectrical transduction: review and perspectives,” *Polymer International*, vol. 59, no. 3, pp. 279–289, Jan. 2010.
- [11] K. W., “Dehnung und Kontraktion bei Änderung der Ionisation eines Netzwerks polyvalenter Fadenmolekülionen,” *Experientia*, vol. 5, no. 8, pp. 318–319, Sep. 1949.
- [12] W. Kuhn, O. Kunzle, and A. Katchalsky, “Verhalten polyvalenter Fadenmolekilionen in Losung,” *Helvetica Chimica Acta*, vol. 31, no. 7, pp. 1994–2037, Sep. 1948.
- [13] W. Kuhn, B. Hargitay, A. Katchalsky, and H. Eisenberg, “Reversible dilation and contraction by changing the state of ionization of high-polymer acid networks,” *Nature*, vol. 165, pp. 514–516, 1950.
- [14] R. Hamlen, C. Kent, and S. Shafer, “Electrolytically activated contractile polymer,” *Nature*, vol. 206, no. 4989, pp. 1149–1150, 1965.
- [15] A. Grodzinsky, “Electromechanics of deformable polyelectrolyte membranes,” Graduate Thesis, 1974.

- [16] A J. Grodzinsky and J. R. Melcher, "Electromechanical transduction with charged polyelectrolyte membranes," *IEEE transactions on bio-medical engineering*, vol. 23, no. 6, pp. 421–433, Nov. 1976.
- [17] M. Shahinpoor, "Conceptual design, kinematics and dynamics of swimming robotic structures using ionic polymeric gel muscles," *Smart Materials and Structures*, vol. 1, no. 1, pp. 91–94, 1992.
- [18] D. Adolf and M. Shahinpoor, "Electrically controlled polymeric gel actuators," *US Patent*, Patent no. 5,250,167, 1993.
- [19] M. Shahinpoor, "Microelectro-mechanics of ionic polymeric gels as artificial muscles for robotic applications," *Robotics and Automation Conf*, vol. 2, pp. 380-385, 1993.
- [20] M. Shahinpoor, "Continuum electromechanics of ionic polymeric gels as artificial muscles for robotic applications," *Smart Materials and Structures*, vol. 3, no. 3, pp. 367–372, 1994.
- [21] M. Shahinpoor and M. S. Thompson, "The Venus Flytrap as a model for a biomimetic material with built-in sensors and actuators," *Materials Science and Engineering: C*, vol. 2, no. 4, pp. 229–233, Sep. 1995.
- [22] M. Mojarrad and M. Shahinpoor, "Ion exchange membrane-platinum composites as electrically controllable artificial muscles," *Proc. 3rd Int. Conf. on Intelligent Materials, ICIM'96, 3rd Eur. Conf. on Smart Structures and Materials (Lyon, 1996)*, vol. 2779, pp. 1012–1017, 1996.
- [23] M. Mojarrad and M. Shahinpoor, "Biomimetic robotic propulsion using polymeric artificial muscles," *Robotics and Automation Conf*, vol. 3, pp. 2152-2157, April, 1997.
- [24] M. Shahinpoor and M. Mojarrad, "Soft actuators and artificial muscles," *US Patent*, Patent no. 6,109,852, 2000.
- [25] M. Shahinpoor and K. J. Kim, "The effect of surface-electrode resistance on the performance of ionic polymer-metal composite (IPMC) artificial muscles," *Smart Materials and Structures*, vol. 9, no. 4, pp. 543–551, Aug. 2000.
- [26] C. Marx, D. Caulfield, and S. Cooper, "Morphology of ionomers," *Macromolecules*, vol. 525, no. 7, pp. 344–353, 1973.
- [27] J. Kao, R. S. Stein, W. J. MacKnight, W. P. Taggart, and G. S. Cargill, "Structure of the Cesium Salt of an Ethylene-Methacrylic Acid Copolymer from Its Radial Distribution Function," *Macromolecules*, vol. 7, no. 1, pp. 95–100, Jan. 1974.
- [28] T. Gierke, G. Munn, and F. Wilson, "Morphology of perfluorosulfonated membrane products," *ACS Symposium Series*, vol. 180, chapter 10, pp. 195–216, 1982.
- [29] T. Gierke and W. Hsu, "The cluster-network model of ion clustering in perfluorosulfonated membranes," *ACS Symposium Series*, vol. 180, pp. 283–307, 1982.
- [30] S. Nemat-nasser and S. Zamani, "Experimental Study of Nafion<sup>TM</sup> and Flemion-based Ionic Polymer-metal Composites (IPMCs) with Ethylene Glycol as Solvent," *EAP Actuators and Devices, SPIE*, pp. 428-435, 2001.
- [31] M. Shahinpoor and K. J. Kim, "Solid-state soft actuator exhibiting large electromechanical effect," *Applied Physics Letters*, vol. 80, no. 18, p. 3445, 2002.

- [32] M. D. Bennett and D. J. Leo, "Ionic liquids as stable solvents for ionic polymer transducers," *Sensors and Actuators A: Physical*, vol. 115, no. 1, pp. 79–90, Sep. 2004.
- [33] S. Liu, R. Montazami, Y. Liu, V. Jain, M. Lin, J. R. Heflin, and Q. M. Zhang, "Layer-by-layer self-assembled conductor network composites in ionic polymer metal composite actuators with high strain response," *Applied Physics Letters*, vol. 95, no. 2, pp. 023505, 2009.
- [34] Y. Liu, R. Zhao, M. Ghaffari, J. Lin, S. Liu, H. Cebeci, R. G. de Villoria, R. Montazami, D. Wang, B. L. Wardle, J. R. Heflin, and Q. M. Zhang, "Equivalent circuit modeling of ionomer and ionic polymer conductive network composite actuators containing ionic liquids," *Sensors and Actuators A: Physical*, vol. 181, pp. 70–76, Jul. 2012.
- [35] T. Okada, G. Xie, O. Gorseth, and S. Kjelstrup, "Ion and water transport characteristics of Nafion membranes as electrolytes," *Electrochimica Acta*, vol. 43, no. 24, pp. 3741–3747, 1998.
- [36] K. Onishi, S. Sewa, K. Asaka, N. Fujiwara, and K. Oguro, "Morphology of electrodes and bending response of the polymer electrolyte actuator," *Electrochimica Acta*, vol. 46, no. 5, pp. 737–743, 2001.
- [37] M Shahinpoor, Y Bar-Cohen, J O Simpson and J Smith, "Ionic polymer – metal composites (IPMCs) as biomimetic sensors , actuators and artificial muscles — a review," *Smart Materials and Structures*, vol. 7, no. 6, pp. R15-R30, 1998.
- [38] R. Montazami, S. Liu, Y. Liu, D. Wang, Q. Zhang, and J. R. Heflin, "Thickness dependence of curvature, strain, and response time in ionic electroactive polymer actuators fabricated via layer-by-layer assembly," *Journal of Applied Physics*, vol. 109, no. 10, pp. 104301, 2011.
- [39] B. J. Akle, D. J. Leo, M. a. Hickner, and J. E. McGrath, "Correlation of capacitance and actuation in ionomeric polymer transducers," *Journal of Materials Science*, vol. 40, no. 14, pp. 3715–3724, Jul. 2005.
- [40] P. Millet, F. Andolfatto, and R. Durand, "Preparation of solid polymer electrolyte composites: investigation of the ion-exchange process," *Journal of applied electrochemistry*, vol. 25, no. 3, pp. 227–232, 1995.
- [41] P. Millet, F. Andolfatto, and R. Durand, "Preparation of solid polymer electrolyte composites: investigation of the precipitation process," *Journal of applied electrochemistry*, vol. 25, no. 3, pp. 233–239, 1995.
- [42] T. Rashid , M. Shahinpoor, "Force optimization of ionic polymeric platinum composite artificial muscles by means of an orthogonal array manufacturing method," *EAP Actuators and Devices*, vol. 3669, SPIE, pp. 289–298, 1999.
- [43] B. Akle, K. Wiles, D. Leo, J. McGrath, "Effects of electrode morphology on the performance of BPSH and PATS ionic polymer transducers," *Proceedings of the EAP Actuators and Devices*. SPIE, paper 5385-73, 2004.
- [44] B. J. Akle and D. J. Leo, "Single-Walled Carbon Nanotubes - Ionic Polymer Electroactive Hybrid Transducers," *Journal of Intelligent Material Systems and Structures*, vol. 19, no. 8, pp. 905–915, Oct. 2008.
- [45] B. J. Akle, M. D. Bennett, D. J. Leo, K. B. Wiles, and J. E. McGrath, "Direct assembly process: a novel fabrication technique for large strain ionic polymer

- transducers," *Journal of Materials Science*, vol. 42, no. 16, pp. 7031–7041, Apr. 2007.
- [46] Lucy Netzer and Jacob Sagiv, "A New Approach to Construction of Artificial Monolayer Assemblies," *American Chemical Society*, Vol. 105, no. 3, pp. 674–676, 1983.
  - [47] G. Decher, "Fuzzy Nanoassemblies: Toward Layered Polymeric Multicomposites," *Science*, vol. 277, no. 5330, pp. 1232–1237, Aug. 1997.
  - [48] G. Decher, J. D. Hong, and J. Schmitt, "Buildup of ultrathin multilayer films by a self-assembly process: III. Consecutively alternating adsorption of anionic and cationic polyelectrolytes on charged surfaces," *Thin Solid Films*, vol. 210–211, part 2, pp. 831–835, Apr. 1992.
  - [49] Yu. Lvov, G. Decher and G. Sukhorukov, "Assembly of Thin Films by Means of Successive Deposition of Alternate Layers of DNA and Poly(allylamine)," *Macromolecules*, vol. 26, no. 20, pp. 5396–5399, 1993.
  - [50] G. Decher, B. Lehr, K. Lowack, Y. Lvov, and J. Schmitt, "New nanocomposite films for biosensors: layer-by-layer adsorbed films of polyelectrolytes, proteins or DNA," *Biosensors and Bioelectronics*, vol. 9, no. 9–10, pp. 677–684, Jan. 1994.
  - [51] P. T. Hammond, "Form and Function in Multilayer Assembly: New Applications at the Nanoscale," *Advanced Materials*, vol. 16, no. 15, pp. 1271–1293, Aug. 2004.
  - [52] F. van Ackern, L. Krasemann, and B. Tieke, "Ultrathin membranes for gas separation and pervaporation prepared upon electrostatic self-assembly of polyelectrolytes," *Thin Solid Films*, vol. 327–329, pp. 762–766, Aug. 1998.
  - [53] J. Leva and T. J. McCarthy, "Poly ( 4-methyl-1-pentene ) -Supported Polyelectrolyte Multilayer Films: Preparation and Gas Permeability," *Macromolecules*, vol. 30, no. 6, pp. 1752–1757, 1997.
  - [54] T. Farhat and J. Schlenoff, "Ion transport and equilibria in polyelectrolyte multilayers," *Langmuir*, vol. 17, no. 4, pp. 1184–1192, 2001.
  - [55] X. Liu and M. Bruening, "Size-selective transport of uncharged solutes through multilayer polyelectrolyte membranes," *Chemistry of materials*, vol. 16, no. 2, pp. 351–357, 2004.
  - [56] J. Harris, L. Jacqueline, and M. Bruening, "Layered polyelectrolyte films as selective, ultrathin barriers for anion transport," *Chemistry of materials*, vol. 12, no. 7, pp. 1941–1946, 2000.
  - [57] J. Lukáš, H. Schwarz, and K. Richau, "Polyelectrolyte complex membranes—surface and permeability properties," *Macromolecular Symposia*, vol. 188, no. 1, pp. 155–165, 2002.
  - [58] Dean DeLongchamp and Paula T. Hammond, "Layer-by-Layer Assembly of PEDOT/Polyaniline Electrochromic Devices," *Advanced Materials*, vol. 13, no. 19, pp. 1455–1459, 2001.
  - [59] D. M. DeLongchamp and P. T. Hammond, "High-Contrast Electrochromism and Controllable Dissolution of Assembled Prussian Blue/Polymer Nanocomposites," *Advanced Functional Materials*, vol. 14, no. 3, pp. 224–232, Mar. 2004.
  - [60] D. M. DeLongchamp and P. T. Hammond, "Multiple-Color Electrochromism from Layer-by-Layer-Assembled Polyaniline/Prussian Blue Nanocomposite Thin Films," *Chemistry of Materials*, vol. 16, no. 23, pp. 4799–4805, Nov. 2004.

- [61] R. Montazami, V. Jain, and J. R. Heflin, "High contrast asymmetric solid state electrochromic devices based on layer-by-layer deposition of polyaniline and poly(aniline sulfonic acid)," *Electrochimica Acta*, vol. 56, no. 2, pp. 990–994, Dec. 2010.
- [62] A. a Mamedov, N. a Kotov, M. Prato, D. M. Guldi, J. P. Wicksted, and A. Hirsch, "Molecular design of strong single-wall carbon nanotube/polyelectrolyte multilayer composites.," *Nature materials*, vol. 1, no. 3, pp. 190–194, Nov. 2002.
- [63] J. H. Rouse and P. T. Lillehei, "Electrostatic Assembly of Polymer/Single Walled Carbon Nanotube Multilayer Films," *Nano Letters*, vol. 3, no. 1, pp. 59–62, Jan. 2003.
- [64] A. P. R. Johnston, C. Cortez, A. S. Angelatos, and F. Caruso, "Layer-by-layer engineered capsules and their applications," *Current Opinion in Colloid & Interface Science*, vol. 11, no. 4, pp. 203–209, Oct. 2006.
- [65] A. L. Becker, A. P. R. Johnston, and F. Caruso, "Layer-by-layer-assembled capsules and films for therapeutic delivery.," *Small (Weinheim an der Bergstrasse, Germany)*, vol. 6, no. 17, pp. 1836–52, Sep. 2010.
- [66] S. Liu, R. Montazami, Y. Liu, V. Jain, M. Lin, X. Zhou, J. R. Heflin, and Q. M. Zhang, "Influence of the conductor network composites on the performance of ionic polymer conductor network composite actuators," *Sensors and Actuators A: Physical*, vol. 157, no. 2, pp. 267–275, 2010.

## CHAPTER 2

### Influence of Conductive Network Composite Thickness on Electromechanical and Mechanoelectrical Performance of Ionic Polymer-Metal Composite Transducer

#### **Abstract**

The important role of the nanostructure of conductive network composite (CNC) layers on the performance of ionic polymer-metal composite (IPMC) transducer has been discussed detailedly. IPMC transducers exhibit both electromechanical and mechanoelectrical behaviors. When subjected to an external electric field, electromechanical behavior of IPMC transducers causes an actuation response which can be reversed by alternation of the polarity of the applied field. The same structure, when subjected to an external mechanical force, generates an electrical signal which can be picked up by ordinary electronic. Mechanoelectrical behavior of IPMCs is utilized in stress sensors and structural health monitoring devices. Incorporation of spherical gold nanoparticles (AuNPs) in the CNC layers can significantly improve the electrical conductivity and porosity of the IPMC transducer, which provides an optimum structure to increase the participation of ions in the actuation and sensing behaviors. We have employed the layer by layer (LbL) self-assembly technique to fabricate CNC layers based on AuNPs and poly(allylamine hydrochloride) (PAH) polycation with a controllable thickness in nano and micro ranges; which, when compared with IPMC transducer without CNC layers on both sides of ionomer membrane, show an improvement in the actuation and sensing performances significantly. Briefly, when applying a voltage across the thickness of IPMC actuator, the net cationic and anionic strains can be enhanced by

almost 400% and 260% respectively when the number of bilayers in CNC increased from 0 (bare Nafion membrane) to 40, which is similar to the results obtained by Montazami and Liu *et.al*[1]. A preferred explanation for this improvement is that a thicker CNC layer has a capacity to store a larger volume of mobile ions. Meanwhile, when compared with the sensor without CNC layers, the generated voltage of the sensor with CNC consisting of 40 bilayers is 1.8 times larger when bending, and 8 times larger when subject to a dynamic impact loading.

## 2.1 Introduction

Due to their unique properties including low cost, low density, ease of processing and sensitive to external stimulus, ionic electroactive polymers (IEAPs) have been extensively studied during the last several decades. To the best of the authors' knowledge, as early as 1950, Kuhn *et.al* reported the very first research results on the ionic chemomechanical deformation of polymers[2]. They found that, if suspended in water, a three-dimensional network containing polyelectrolytes such as polyacrylic acid (PAA) or polyvinyl chloride (PVA) systems, can contract and dilate reversibly upon alternating addition of small amounts of acid and alkali to the medium. They also pointed out that the shape of ionizable polymeric molecules depends on the number of charges distributed over the molecular chain. Also, Hamlen *el.tal* showed that another typical system based on a PVA-PAA co-polymer, also exhibited dimension change in response to an applied voltage since its chemical environment will become either acidic or alkaline depending on the direction of the current[3]. From there on, considerable attention has been paid on the potential application of ionic electroactive polymers, and these works provided a firm platform for the further studies on ionomeric polymer transducers.

Among IEAPs, IPMC is one of the most extensively studies class during the last two decades due to a number of promising characteristics and their potential applications in industry, advanced structure and biomedical devices. IPMC transducers, also known as ionomeric polymer transducers, are a class of electroactive polymers that are able to operate as both electromechanical actuators and mechanoelectrical sensors[4]. Briefly, IPMC is a structure based on ionic electroactive polymers that bends in response to an electrical activation or generates electromotive voltage when under mechanical stress. IPMCs usually consist of a thin ionomer membrane (usually Nafion, or Flemion) with typical thickness of approximately 100  $\mu\text{m}$ [5]. Two thin layers of noble metal electrodes such as platinum or gold are coated on the two sides of the ionomer membrane. Due to the fixed anions on the backbone of the polymer membrane, same amount of cations (typically  $\text{Na}^+$ ,  $\text{K}^+$ ,  $\text{Li}^+$  and  $\text{Cs}^+$  in water solution) also exists in the membrane and can move freely with the existence of polyelectrolyte[5]. Ionic liquids (ILs) have been investigated as possible new electrolytes for IPMC transducers due to their higher electrical stability and very low (near zero) vapor pressure when compared with aqueous electrolytes[6].

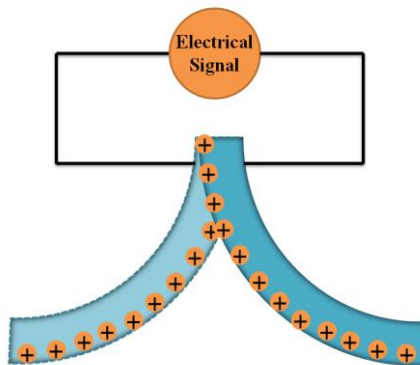


**Fig. 2.1 Schematic representation of an IPMC transducer; as actuator, the IPMC will bend under an electrical signal; as sensor, the IPMC will generate an electrical signal in response to mechanical stress.**

Illustrated in Fig.2.1 is a schematic representation of IPMC electromechanical and mechanoeletrical process. For actuation process, an applied electrical signal leads to attraction and repulsion of ions toward and away from electrodes of opposite and alike charge, respectively. Accumulation of mobile ions at cathode and anode of the IPMC causes a mechanical imbalance which in turn results in an actuation response. Actuator response to a wave function is shown in Fig. 2.1. When under mechanical stress, mobile ions are displaced in the IPMC structure. Motion of charged particles (ions) results in generation of an electrical signal which can be sensed by ordinary electronics[5]. Experimental results indicated that a higher population of excess charges at the electrodes is preferred for both actuation and sensing mechanisms[7–9]. Porous electrodes which can provide higher interface areas between the electrolyte and transducer have been adopted during the transducer design and fabrication process. Usually, two conductive network composite (CNC) layers are deposited on the two sides of the ionic polymer membrane to improve the porosity and act as reservoirs for electrolyte.

A widely used method at earlier studies is plating metal cation complex onto the ionomeric membrane surface at first, then nanosized metal particles would be obtained by chemical reduction method for penetration into the ionomeric membrane[8–10]. In this method, the interfacial area between the polymer and the metal is very large, which is beneficial for the formation of porous electrodes and a larger capacitance of these devices. Later a novel method on the manipulating of electroding process, direct assembly process (DAP), has been proposed by Akle and Leo[5–7, 11, 12]. They mixed an ionic polymer solution such as Nafion with conductor nano-particles and deposited the mixture on the Nafion membrane as an electrode. This method significantly increases the

effective interfacial area and thus the capacitance of electrodes; and allows use of a large range of conductive nanosized powders in the fabrication of IPMC, including non-metals such as carbon nanotubes[12]. More recently, another attractive class of CNC layers via layer by layer (LbL) self-assembly technique in manufacture of ionic polymer conductor network composite(IPCNC) is provided by Montazami and Liu *et.al*[1, 13-15]. Experimental results show that a better electromechanical behavior of IPMC actuators with CNC layers through LBL technique can be obtained, which is led by the formation of porous electrodes and a larger electrolyte uptake capacity due to the high porosity of CNC layers.

Briefly, LbL self-assembly deposition, is a nanofabrication technique based on use of oppositely charged polyelectrolytes, DNA, conducting polymers, proteins, and metal or semiconductor nanoparticles. Precise control over the thickness along with the high porosity of fabricated films make LbL fabrication technique widely applicable to fabrication of IPMC actuators and sensors. Our working hypothesis is that by LbL self-assembly technique, uniform CNC layers can be obtained and the thicker CNC layer has a capacity of containing more mobile ions, which can improve the actuation and sensing behaviors of IPMC transducers. The objective of this work is to fabricate a series of IPMC transducers with different CNC layers and investigate the influence of CNC thickness on electromechanical and mechanoelectrical performance. Different CNC layers are fabricated via LbL self-assembly technique and the thickness can be controlled by the deposited number of bilayers. As will be presented, experimental results demonstrated that the presence of CNC layers in IPMC transducers significantly improve the actuation and sensing behaviors; a thicker CNC layer has a structure with higher

electrical conductivity and the capacity of containing larger amount of polyelectrolytes, which is beneficial for the improvement in the performance of IPMC transducers.

## 2.2 Experimental section

### 2.2.1 The fabrication of IPMC transducer

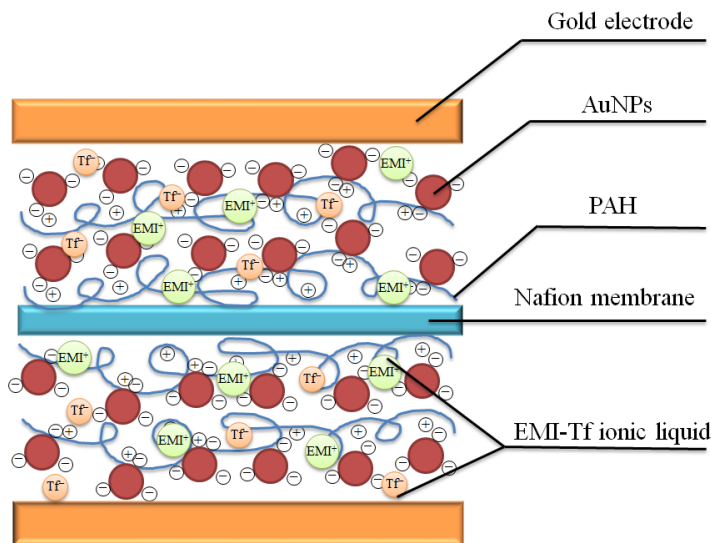


**Fig. 2.2 Schematic representation of the transducer structure with CNC layers via LBL self-assembly deposition.**

The ionomer membrane of IPMC transducer investigated in this work was Nafion membrane NR 211 with 25  $\mu\text{m}$  thickness which is commercially-available from Ion Power, Inc. Two CNC layers were deposited on the two sides of Nafion membrane to improve the porosity of electrodes via LBL self-assembly technique. Briefly, Nafion film attached on a glass frame was alternately exposed to 10 mM polycation poly(allylamine hydrochloride) (PAH, Sigma Aldrich) and 20 ppm gold nanoparticles (AuNPs,  $\sim 3\text{nm}$  diameter, Purest Colloids, Inc.) for 5 min each. After every exposure, three times rinsing step was required in deionized (DI) water for 1 min each to avoid contamination. One whole cycle consists of exposure to PAH solution, 3 rinsing steps, exposure to AuNPs solution, and 3 rinsing steps, which forms one AuNPs/PAH bilayer. 10, 20, 30, and 40

AuNPs/PAH bilayers were obtained for the consideration of the thickness effects on the transducer performance.

After deposition of AuNPs/PAH CNC layers on both sides of Nafion membrane, the coated membrane was then soaked in 1-ethyl-3-methylimidazolium trifluoromethanesulfonate (EMI-Tf) (Sigma Aldrich) ionic liquid at 80 °C to achieve 40wt% ionic liquid intake. After removal of the redundant EMI-Tf ionic liquid on the surface, two gold leaves (L.A. Gold Leaf) of 50 nm thickness (each) were hot-pressed on both sides of the membrane at 120 kN pressure for 40 seconds to get IPMC transducer. A schematic structure of the transducer is shown in Fig. 2.2. Fig. 2.3 is an SEM image of a 20-bilayer AuNP surface, showing a uniform and homogeneous CNC layer surface.

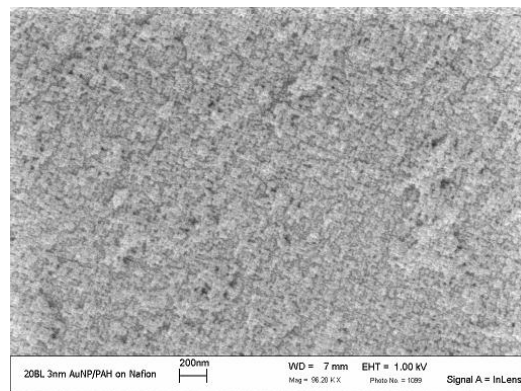


**Fig. 2.3 SEM image of 20 bilayers of AuNPs/PAH on Nafion.**

### 2.2.2 Characterization of samples

The thickness of different components of a set of transducers consisting of different number AuNPs/PAH bilayers was measured by a contact profilometer. The results are represented in Table 2.1. Bare Nafion and each gold electrode is 25 µm and 50 nm thick respectively. The thickness of CNC layers with respect to the number of deposited bilayers exhibits a linear growth of approximate 2 nm/bilayer.

**Table 2.1**Thickness of different components of variety of transducers.

Sample	CNC ( $\mu\text{m}$ )	Transducer ( $\mu\text{m}$ )
<b>Bare Nafion</b>	0.000	25.100
<b>10 bilayers</b>	0.023	25.146
<b>20 bilayers</b>	0.042	25.184
<b>30 bilayers</b>	0.064	25.228
<b>40 bilayers</b>	0.081	25.262

Optical spectrum was acquired using PerkinElmer Lambda-25 UV/VIS Spectrometer. The CNC layer surface morphology was measured by Dino-Lite digital microscopy. The surface resistance of the CNC layers with different number of AuNPs/PAH bilayers is measured by Jandel four-point-probe measurement system. The electrical characteristics were measured in air by Princeton Applied Research VersaSTAT 4 at 2-electrode setting. The actuation motion of the actuators was recorded by a charge couple device camera attached to an in-house fabricated probe station for the later strain calculation and image analysis. The applied voltage was generated by a dual channel arbitrary function generator. The maximum applied voltage is 4V and digital phosphor oscilloscope was used to monitor and record the applied voltage. For the actuation performance measurement, one end of the bending sample was fixed by two titanium lines which also acted as electrodes to conduct generated electrical signal, and the radius of curvature or tip displacement of the free end was recorded to calculate the bending strain. Usually two different methods were used to calculate the bending strain depending on the extent of bending[14]. While equation (a) is used in the case of large bending with  $r$  representing the radius of curvature depending on the extent of bending and  $h$  representing the thickness of the actuators, equation (b) is adopted to calculate small,

vibration-like bending where  $\delta$  representing the tip displacement of the free end and  $L$  representing the free length of actuator [16]. In this work, the strain caused by cations or anions is larger enough to be calculated by equation (a). The strain calculated with these two equations is the net strain.

$$\varepsilon(\%) = \frac{h}{2r} \times 100 \quad (a)$$

$$\varepsilon(\%) = \frac{\delta h}{L^2} \times 100 \quad (b)$$

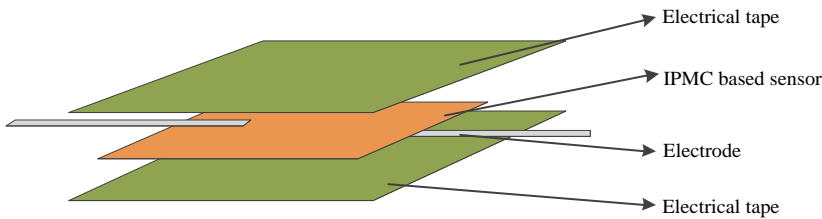


**Fig. 2.4 Schematic representation of the sample to be tested for quasi-static and dynamic sensing response.**

When investigation sensing performance, quasi-static and dynamic sensing response in the form of electrical signal was investigated in this work. As shown in Fig. 2.4, the strip ( $15\text{mm} \times 7\text{mm}$ ) of IPMC was covered between two electrical tapes with copper as electrodes, connecting to the digital phosphor oscilloscope to record the generated voltage.

### 2.3 Results and discussion

#### 2.3.1 Characterization of CNC layers in IPMC

The CNC layers formation process via LBL deposition was characterized by UV-Vis spectroscopy, which provides information on the thickness difference due to different number of bilayers. The UV-Vis absorbance spectra of up to 10 bilayers of AuNPs/PAH formed by LbL assembly are shown in Fig.2.5(a) while Fig. 2.5(b) shows the digital

microscopy images of the surface morphology of different bilayers comprising CNC.

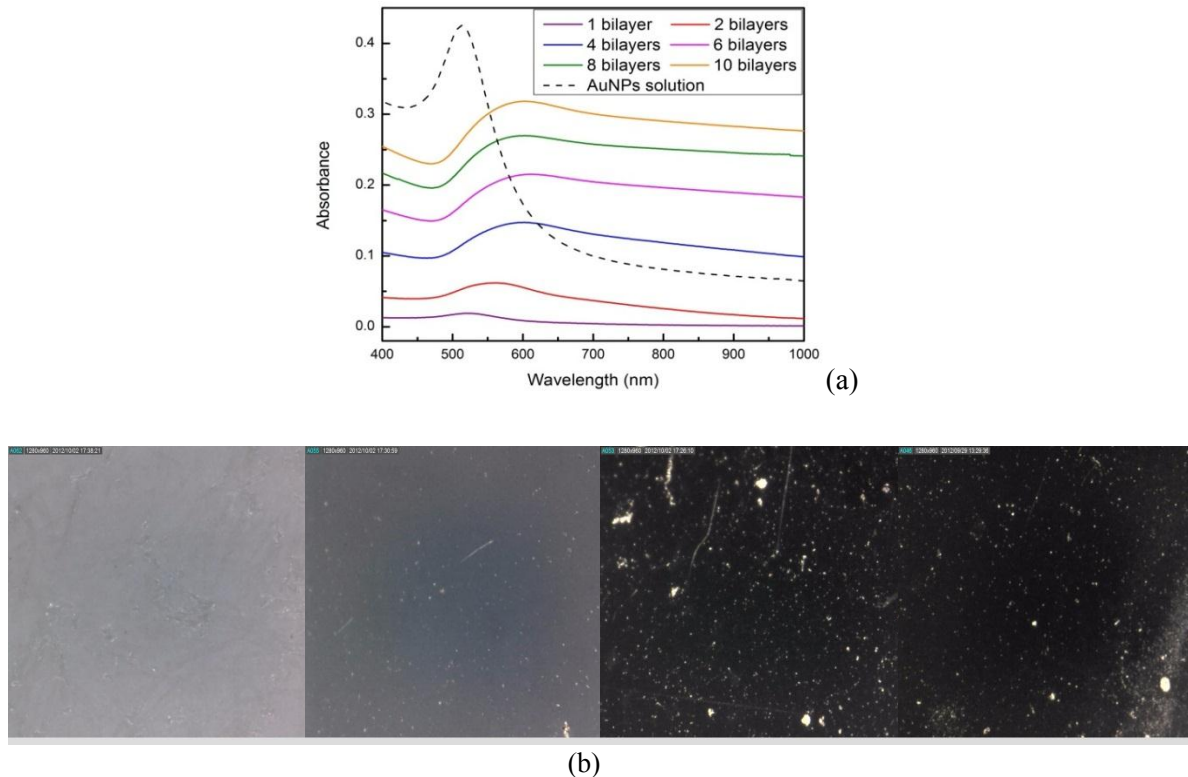


**Fig. 2.5 (a)** UV-Vis absorbance spectrum of growing process of AuNPs/PAH thin-film. **(b)** Digital microscopy images for different number of bilayers of AuNPs/PAH (left to right 10, 20, 30 and 40 bilayers).

In this work, 10mM PAH solution was used as partner polyelectrolyte to form the first layer on a negative-charged Nafion membrane via ionic attraction, which acted as the foundation for the formation of AuNPs layer. These steps form one bilayer, and the exact formation process of AuNPs/PAH thin-film from 0 bilayer to 10 bilayers was distinctly described in Fig. 2.5(a). After each successive adsorption of one or two bilayers, the absorbance spectrum of the resulted CNC layers was recorded. Since the AuNPs/PAH thin-film are fabricated on both sides of the substrate, each absorbance line represents twice the peak intensity. The buildup of porous CNC layers structure was demonstrated by the increase in the AuNPs surface plasmon band located at around 515

nm. It is also noticeable that when compared with the UV-Vis spectrum of AuNP solution at 20 ppm concentration (represented with dash line), a shift toward higher wavelength of the absorption band around 590 nm was also observed, which may be attributed to the strong electromagnetic coupling between neighboring nanoparticles[17]. The increase of peak intensity as the number of bilayers increases, demonstrated a well-packed, homogenous AuNPs/PAH multilayers has been attained in the CNC via LBL self-assembly deposition. This result can also be confirmed by the digital microscopy images. Increasing the number of bilayers, as shown in Fig. 2.5(b), results in a darker color. As the increase of peak intensity shown in (a), they both led by a larger amount of AuNPs deposition in the CNC layers. All films consisting of different number of bilayers shown have a uniform and homogeneous surface.

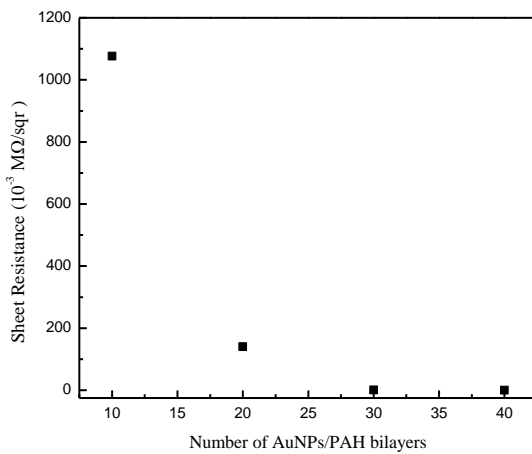


**Fig. 2.6 Sheet resistance decreases significantly as the number of AuNPs/PAH bilayers increased.**

Typically, CNC layers are designed to act as reservoirs for electrolyte solution during the fabrication of IPMC transducers. The mobility of ions through CNC defines the attributes of CNC layers and can ultimately define the IPMC transducer performance. Usually the mobility of ions depends on many factors including the nano\micro-channels

as well as the interaction of ions with the nano\micro-channels[1]. An optimum structure of the CNC layers in IPMC transducer should have a dense enough electrically conductive structure to promote the participation of ions distributed in the Nafion membrane and CNC layers while in the presence of an electric field or an applied deformation[14].

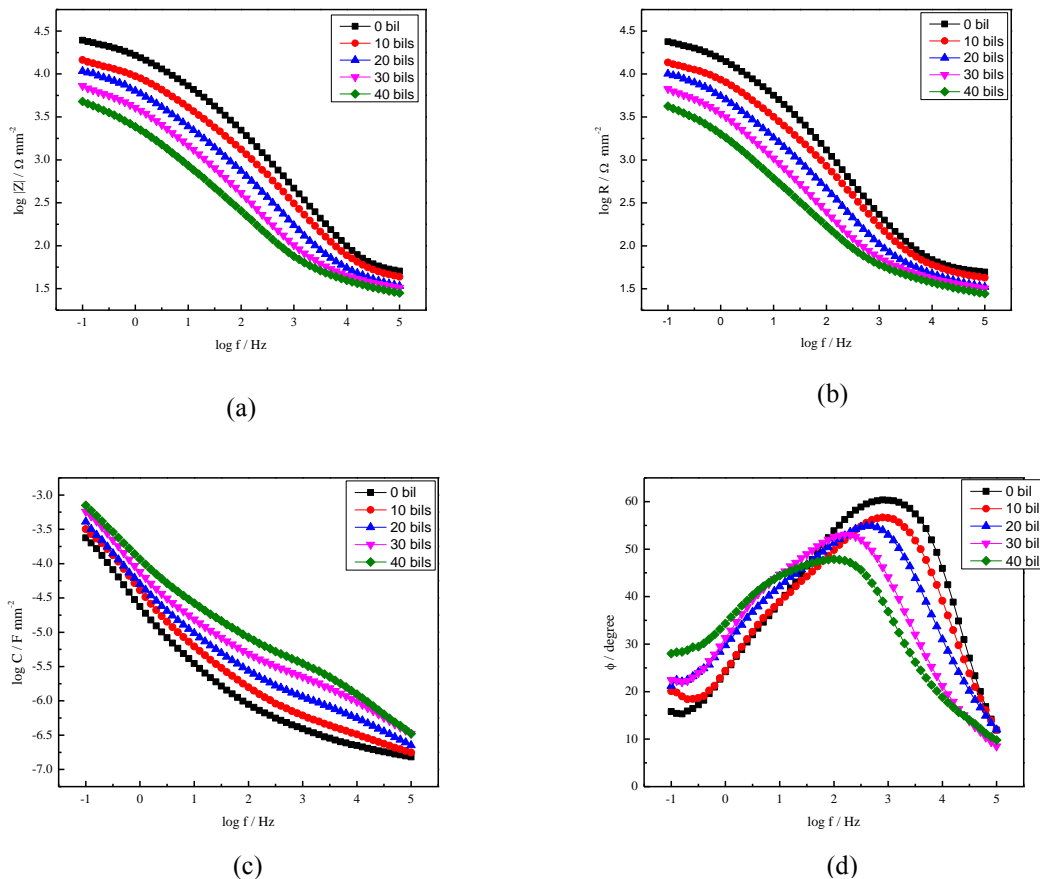


**Fig. 2.7 Electrical impedance of IPMC actuators with different number of bilayers comprising the CNC.**

Considering the unique geometry of CNC layer, while its thickness is much smaller than its planar area, we use four-point-probe method to measure the sheet resistance of samples consisting of different number of bilayers, the result are shown in Fig.2.6. As expected, the sheet resistance decreases significantly as number of AuNPs/PAH bilayers

increased from 10 to 40. While the existence of PAH does not have significant contribution to the electrical conductivity of CNC, the increasing conductivity is due to a higher concentration and a higher interconnectivity of the conductive gold nanoparticles as the number of AuNPs/PAH bilayers increases from 10 to 40. It has been observed that a better electrically conductive structure is preferred since it can promote the motion of ions through the CNC layer when an electric field is applied and thus enhance the ultimate performance of IPMC transducer.

Electrical impedance of IPMC transducer as a function of frequency under AC signal was characterized and the results are shown in Fig. 2.7. The goal of this test is to probe the effect of different numbers of bilayers in CNC on the frequency response of transducer. Recall that the electrical impedance can be expressed as

$$Z = Z_{\text{re}} + Z_{\text{im}} = R + \frac{1}{j\omega C}$$

where  $Z_{\text{re}}$  is the real part of the impedance representing resistance  $R$  and  $Z_{\text{im}}$  is the imaginary part representing reactance, in which  $C$  is the capacitance and  $\omega$  is the angular frequency equal to  $2\pi f$  ( $f$  is the frequency). Phase angle  $\phi$  of the electrical impedance is introduced to give the phase difference between voltage and current; where  $\phi = \arctan(1/\omega RC)$ . Resistance and reactance together determine the magnitude of the impedance  $|Z|$ :

$$|Z| = \sqrt{R^2 + (\omega C)^{-2}}$$

Fig. 2.7 represents the relationship of  $|Z|$ ,  $R$ ,  $C$  and  $\phi$  (shown in (a), (b), (c) and (d) respectively) versus the frequency  $f$  from 0.1 Hz to 100,000 Hz. In fact, the electromechanical responses of IPMC actuator occur at low frequency range, often at the range below 10 Hz, while the mechanoeletrical responses of IPMC sensor often occur at

the frequency range below 100 Hz, we prefer to focus on the impedance response versus low frequency range. Fig. 2.7 (a)-(c) indicate that when the number of bilayers in CNC increases from 0 (bare Nafion membrane) to 40, the magnitudes of the impedance  $|Z|$  and resistance  $R$  decrease while the capacitance  $C$  increases at the low frequency range, meaning that a thicker CNC layer consisting of higher number of bilayers has a larger capacitive component when compared with other samples in this set. It can also be confirmed by Fig. 2.7(d), which represents the phase angle as a function of frequency. By definition,  $\phi = 90^\circ$  corresponds to a pure capacitor and  $\phi = 0^\circ$  to a pure resistor. Since the resistive component represents the electrical loss, we prefer an IPMC transducer demonstrating a larger phase angle  $\phi$  to obtain a high electrical efficiency [13]. Fig. 2.7(d) indicates that the phase angle  $\phi$  increases with the increase of number of bilayers in CNC. The highest phase angle corresponds to the sample with CNC consisting of 40 bilayers, confirming the highest capacitive component proportion and the highest electrical efficiency.

### **2.3.2 Characterization of actuation performance in IPMC**

As have been showed previously by Montazami and Liu *et.al*[1, 14], the IPMC-based actuator with EMI-Tf ionic liquid as electrolyte first exhibits a fast and small bend toward the anode led by the quick motion of  $\text{EMI}^+$  cations; then this quick and small cationic strain is canceled by another slow and more effective bending strain toward the cathode led by the moving  $\text{Tf}^-$  anions and/or anionic complexes. It is believed that the more effective anionic strain is led by the charge clusters of negative net charge (e.g.  $\text{Tf}^- \text{-} \text{EMI}^+ \text{-} \text{Tf}^-$ ) existence in the ionic liquid electrolyte[14, 18]. Fig. 2.8 is photographic images of an IPMC-based actuator with 30 bilayers of AuNPs/PAH in CNC, from which

we can find that a more effective anionic strain was obtained after a relative smaller cationic strain when a 4V voltage was applied. Since the strains caused by samples in this work are large enough, equation (a) was used for the calculation and the strain versus number of bilayers in CNC is shown in Fig. 2.9(a). The corresponding actuation curvature Q was also obtained by the inverse of bending radius; the results are shown in Fig. 2.9(b).

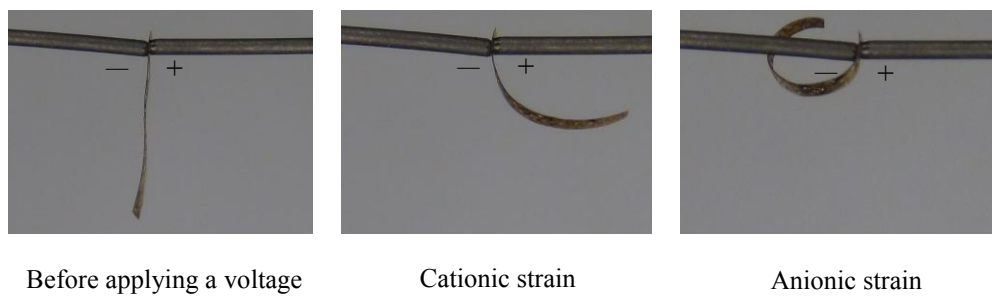


**Fig. 2.8 Photographic images of an IPMC-based actuator with 30 bilayers of AuNPs/PAH in CNC; electrode on the right side is anode.**

Fig. 2.9(a) shows the maximum actuation strains toward the anode and cathode increase linearly with the number of bilayers in CNC at the rates of  $0.0082 \text{ mm}^{-1}/\text{bilayer}$  and  $0.0137 \text{ mm}^{-1}/\text{bilayer}$ , respectively. When the number of AuNPs/PAH bilayers increases from 0 (bare Nafion membrane) to 40, the cationic strain and anionic strain have been enhanced by more than 400% and 260% respectively. Since bending time due to cationic motion is limited because of the subsequent anionic strain to the opposite direction, the larger cationic strain generated by CNC with larger number of AuNPs/PAH bilayers indicates that  $\text{EMI}^+$  cations move quicker in the actuator with thicker CNC when compared with the actuator consisting of CNCs of smaller thickness. A convincing explanation is that a CNC layer with higher bilayer number indicates a higher electrical conductivity in the structure, which is also proved by the sheet resistance results above. Typically, a higher electrical conductive structure can maximize CNC-ion interface,

which will reduce the screening of electric field by ions that have already moved into the CNC at any given time and thus can increase the participation of ions in the actuation process[14]. The increase of anionic strain as a function of number of bilayers is due to the accumulation of a larger number of ions in the thicker CNC since it is capable of containing more electrolyte and hence generating a larger volume imbalance between the electrodes; as a result, a larger mechanical deformation will be obtained[1]. The corresponding curvature also demonstrates a linear relationship with the number of bilayers, which reconfirms the conclusion above.

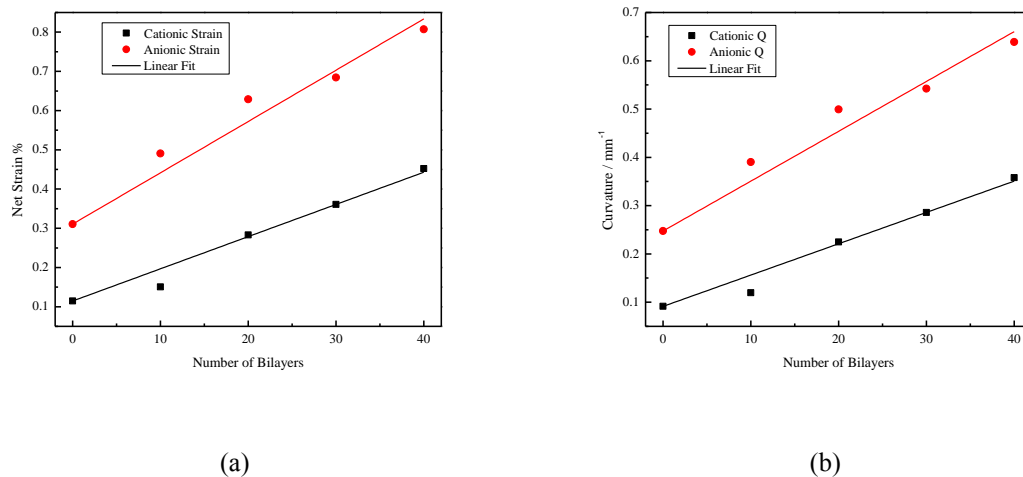


**Fig. 2.9 (a) Net cationic and anionic strains, and (b) cationic and anionic actuation curvatures increase linearly with the increase in the number of bilayers in CNC.**

### 2.3.3 Characterization of sensing performance in IPMC

As early as 1992, investigation of the use of ion-exchange-membrane materials as sensors was carried out by Sadeghipour *et.al*, in which they developed a prototype accelerometer cell by using such ion exchange membrane as a pressure sensor/damper in a small chamber[19]. However, it was Shahinpoor *et.al* who first focused on the application of ionic polymeric gel sensors for quasi-static or dynamic displacement

sensing[20]. They reported both theoretically and experimentally, that mechanically induced nonhomogeneous deformations of such ionic polymeric gels can produce an electric field and the associated voltage. Basically, when IPMC based sensor is bent a stress gradient is built on the outer fibers relative to the neutral axis, then the mobile ions will prefer to shift to their favored region where opposite charges are available[10]. In this work, two samples were used for the sensing test, where sample 1 is IPMC sensor with 0 bilayer of AuNPs/PAH in CNC (bare Nafion membrane) and sample 2 is IPMC sensor with 40 bilayers of AuNPs/PAH in each CNC layer on both sides of the Nafion membrane. For the quasi-static sensing test, the samples were covered between two electrical tapes with copper as electrode connecting to the digital phosphor oscilloscope to record the generated electrical signal; then two samples were bent to the same angle (180 degree) as shown in Fig.2.10 below. The generated electrical signal is represented in Fig. 2.11 and the experimental result showed that when same mechanical bending is applied, sample 2 generates a significantly larger electrical signal. When compared with the signal generated by sample 1, the strength increased by more than 1.8 times. As discussed in section 2.3.2, the larger signal strength is induced by a higher storage capacity of a thicker CNC layers in IPMC sensor. Usually a higher number of bilayers indicates a thicker CNC layer and the ability of containing more electrolytes; and hence more movable ions can shift toward the favored region when a mechanical deformation is applied. Also, a thicker AuNPs/PAH CNC layer has a more compact electrical conductive structure, which is beneficial to reduce the screening of electric field by ions having already moved into CNC[14]. As a result, a larger number of ions will accumulate at the electrodes of opposite charge, which can generate an electrical signal of larger strength.

This result also confirms that a thin and uniform CNC layer fabricated by LbL technique has a rewarding effect on the IPMC sensing performance.

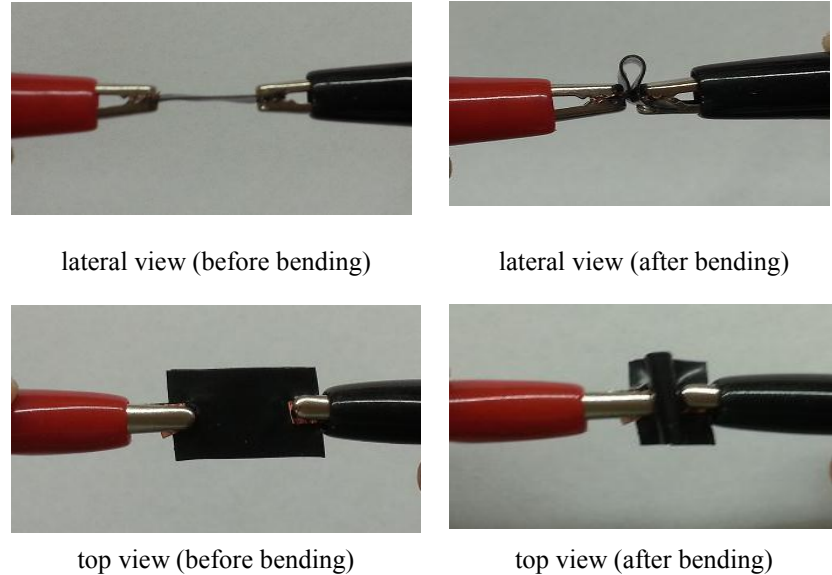


**Fig. 2.10 IPMC based sensor covered between two electrical tapes with Cu as electrode for bending deformation. Top line are lateral views before and after bending; bottom line are corresponding top views.**

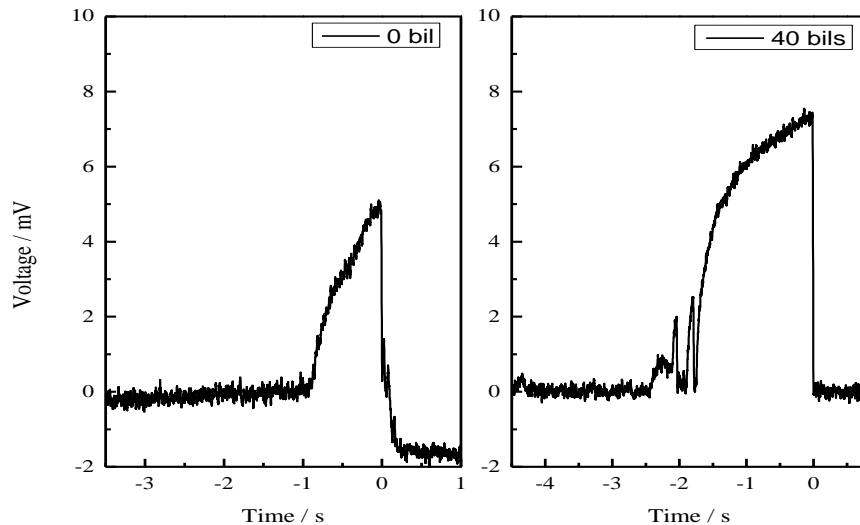


**Fig. 2.11 IPMC sensor response in the form of output voltage when IPMC sensor is subject to a bending deformation. Left is the output voltage from sample 1 and the right is the output voltage from sample 2.**

Moreover, the strips of IPMC sensor are dynamically disturbed by a dynamic impact led by a motor with a constant vibration frequency and the generated electrical

signal is represented in Fig. 2.12.

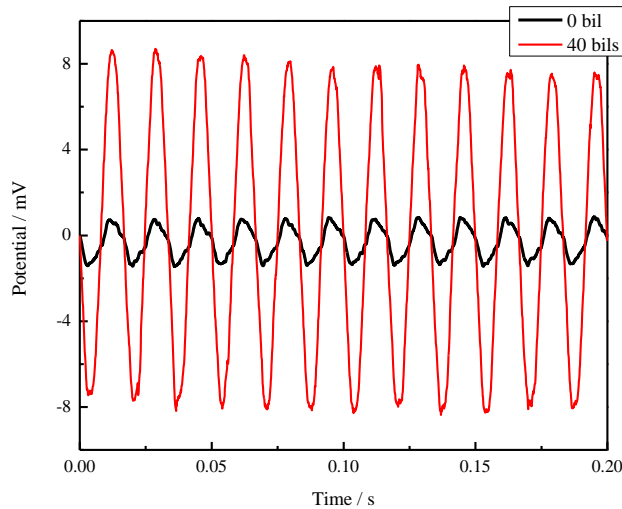


**Fig. 2.12 IPMC sensor response in the form of output voltage when IPMC sensor is subject to a dynamic vibration impact by a motor. Black line represents the output voltage from sample 1 and red line represents the output voltage from sample 2.**

Black line represents the electrical signal generated by sample 1 while red line corresponds to the voltage from sample 2. The dynamic response was observed to be highly repeatable with a fairly band width to 60 Hz for both sample 1 and sample 2, indicating that the time required for mobile ions to travel through CNC is negligible compared to the time required for traveling through the Nafion membrane[1]. Another point needs to be noticed is that although the signal frequency is kept the same for both two samples, the amplitude of the signal of sample 2 exhibits enhancement of more than 8 times (3 folds) when compared with the signal generated by sample 1, reconfirm the conclusion that a thicker CNC layer can store more mobile ions and the larger CNC-ion interface can promote the participation of ions.

## 2.4 Conclusion

We have developed the IPMC transducer with different number of bilayers

comprising CNC layers. LbL self-assembly technique was adopted to control the thickness of CNC layers in nano and micro ranges. With the increased number of bilayers, the sheet resistance decreases significantly, meaning a structure with enough electrical conductivity can be obtained and thus increase the participation of ions in the actuation and sensing performance. Also, we believe that a thicker CNC layer has the capacity to store more mobile ions. Experimental results indicate that this set of actuators with thicker CNC layers are capable of generating larger mechanical deformation for both cationic strain and anionic strain. When the number of AuNPs/PAH bilayers increases from 0 (bare Nafion membrane) to 40, the cationic strain and anionic strain have been enhanced by more than 400% and 260%; its generated voltage has also been improved significantly when the IPMC sensor is applied for quasi-static or dynamic impact loading. The improved actuation and sensing performance achieved in this work is believed as a result of successful fabrication of an appropriate structure of CNC layer. More detailed analysis for time dependence of sensing process and experimental verification are future works.

## Reference

- [1] R. Montazami, S. Liu, Y. Liu, D. Wang, Q. Zhang, and J. R. Heflin, "Thickness dependence of curvature, strain, and response time in ionic electroactive polymer actuators fabricated via layer-by-layer assembly," *Journal of Applied Physics*, vol. 109, no. 10, pp. 104301, 2011.
- [2] W. Kuhn, B. Hargitay, A. Katchalsky, and H. Eisenberg, "Reversible dilation and contraction by changing the state of ionization of high-polymer acid networks," *Nature*, vol. 165, pp. 514–516, 1950.
- [3] R. Hamlen, C. Kent, and S. Shafer, "Electrolytically activated contractile polymer," *Nature*, vol. 206, no. 4989, pp. 1149–1150, 1965.
- [4] M. D. Bennett, D. J. Leo, G. L. Wilkes, F. L. Beyer, and T. W. Pechar, "A model of charge transport and electromechanical transduction in ionic liquid-swollen Nafion membranes," *Polymer*, vol. 47, no. 19, pp. 6782–6796, Sep. 2006.
- [5] D. Pugal, K. Jung, A. Aabloo, and K. J. Kim, "Ionic polymer-metal composite mechanoelectrical transduction: review and perspectives," *Polymer International*, vol. 59, no. 3, pp. 279–289, Jan. 2010.
- [6] M. D. Bennett and D. J. Leo, "Ionic liquids as stable solvents for ionic polymer transducers," *Sensors and Actuators A: Physical*, vol. 115, no. 1, pp. 79–90, Sep. 2004.
- [7] B. J. Akle, D. J. Leo, M. a. Hickner, and J. E. McGrath, "Correlation of capacitance and actuation in ionomeric polymer transducers," *Journal of Materials Science*, vol. 40, no. 14, pp. 3715–3724, Jul. 2005.
- [8] S. Nemat-Nasser and Y. Wu, "Comparative experimental study of ionic polymer–metal composites with different backbone ionomers and in various cation forms," *Journal of Applied Physics*, vol. 93, no. 9, pp. 5255–5267, 2003.
- [9] K. Onishi, S. Sewa, K. Asaka, N. Fujiwara, and K. Oguro, "Morphology of electrodes and bending response of the polymer electrolyte actuator," *Electrochimica Acta*, vol. 46, pp. 737–743, 2001.
- [10] M. Shahinpoor, "Ionic polymer-metal composites (IPMCs) as biomimetic sensors, actuators and artificial muscles-a review," *Smart Materials and Structures*, vol. 7, no. 6, pp. R15–R30, 1998.
- [11] B. Akle, K. Wiles, D. Leo, J. McGrath, "Effects of electrode morphology on the performance of BPSH and PATS ionic polymer transducers," *Proceedings of the EAP Actuators and Devices*. SPIE, paper 5385-73, 2004.
- [12] B. J. Akle and D. J. Leo, "Single-Walled Carbon Nanotubes -- Ionic Polymer Electroactive Hybrid Transducers," *Journal of Intelligent Material Systems and Structures*, vol. 19, no. 8, pp. 905–915, Oct. 2008.
- [13] S. Liu, R. Montazami, Y. Liu, V. Jain, M. Lin, X. Zhou, J. R. Heflin, and Q. M. Zhang, "Influence of the conductor network composites on the electromechanical performance of ionic polymer conductor network composite actuators," *Sensors and Actuators A: Physical*, vol. 157, no. 2, pp. 267–275, 2010.
- [14] R. Montazami, D. Wang, and J. Heflin, "Influence of conductive network composite structure on the electromechanical performance of ionic electroactive polymer actuators," *International Journal of Smart and Nano materials*, vol. 3, no. 3, pp. 204–213, 2012.

- [15] S. Liu, R. Montazami, Y. Liu, V. Jain, M. Lin, J. R. Heflin, and Q. M. Zhang, “Layer-by-layer self-assembled conductor network composites in ionic polymer metal composite actuators with high strain response,” *Applied Physics Letters*, vol. 95, no. 2, p. 023505, 2009.
- [16] B. J. Akle, M. D. Bennett, D. J. Leo, K. B. Wiles, and J. E. McGrath, “Direct assembly process: a novel fabrication technique for large strain ionic polymer transducers,” *Journal of Materials Science*, vol. 42, no. 16, pp. 7031–7041, Apr. 2007.
- [17] X. Hu, W. Cheng, T. Wang, Y. Wang, E. Wang, and S. Dong, “Fabrication, characterization, and application in SERS of self-assembled polyelectrolyte-gold nanorod multilayered films.,” *The journal of physical chemistry. B*, vol. 109, no. 41, pp. 19385–9, Oct. 2005.
- [18] J. Hou, Z. Zhang, and L. a Madsen, “Cation/anion associations in ionic liquids modulated by hydration and ionic medium.,” *The journal of physical chemistry. B*, vol. 115, no. 16, pp. 4576–82, Apr. 2011.
- [19] K. Sadeghipour, “Development of a novel electrochemically active membrane and’smart’material based vibration sensor/damper,” *Smart Materials and Structure*, vol. 1, no. 2, pp. 172–179, 1992.
- [20] M. Shahinpoor, “A new effect in ionic polymeric gels: the ionic flexoelectric effect,” *Proc. SPIE*, vol. 2441, pp. 42–53, 1995.

## CHAPTER 3

### **Ionic Effect of Sodium Chloride on the Conductive Network Composite Nanostructure and its Influence on the Performance of Ionic Polymer-Metal Composite Transducers**

#### **Abstract**

Layer by Layer (LbL) self-assembly technique has been adopted as a new method for the fabrication of conductive network composite (CNC) in ionic polymer-metal composite (IPMC) transducer. A significant improvement in performance of IPMC transducers has been achieved by adopting spherical gold nanoparticles (AuNPs) and poly(allylamine hydrochloride) (PAH) polycation porous thin-films via LbL self-assembly deposition on Nafion. Experimental results demonstrate that the thickness and conformation of CNC nanostructure can be adjusted by the addition of small salt molecules. The presence of salt ions can affect the conformation of polymer chains and their molecular shape since it screens the repulsive force among the same charges on the repeat units of polyelectrolyte. As a result, the polymer chains become more coiling when dissolved in an environment with high ionic strength. Moreover, while part of the charges have been screened, larger amount of polymer chains or nanoparticles are required to reverse the surface charge led by the previous layer. The presence of salt ions in CNC can also prohibits the aggregation of AuNPs and promote a more homogeneous distribution of the nanoparticles. In this case, both the thickness and conformation of CNC have been changed; which, as indicated by experimental results, has a positive influence on the actuation and sensing performance of IPMC devices. Briefly, the cationic curvature increased linearly with the increased number of bilayers at the rate of  $0.0078\text{mm}^{-1}/\text{bilayer}$ .

after the addition of salt, larger than the increasing rate before the addition of salt ( $0.00648 \text{ mm}^{-1}/\text{bilayer}$ ); for the corresponding anionic curvature, the increasing rate has been enhanced from 0.01032 to  $0.01819 \text{ mm}^{-1}/\text{bilayer}$ . Meanwhile, an improved voltage has also been observed when IPMC sensor is bent or subject to a dynamic impact loading, indicating an enhanced sensor function of IPMC has been achieved while the ionic strength is increased.

### 3.1 Introduction

IPMC is one of the most extensively studied class of materials during the last two decades due to a number of promising characteristics and their potential application in the areas such as soft robotic actuators, artificial muscles and dynamic sensors[1–8]. Briefly, IPMC is a structure based on ionic electroactive polymers that bends in response to an electrical activation or generates electromotive voltage when under mechanical stress. IPMCs usually consist of a thin ionomer membrane with thickness usually no larger than  $100 \mu\text{m}$ . Nafion (DuPont) is one of the most common used ion-exchange membrane as well as Teflon or Flemion. Then two thin layers of noble metal electrodes such as platinum or gold are coated on both sides of membrane. Usually, two CNC layers are deposited between the two sides of the ionomer membrane and the electrodes to improve the porosity of electrodes and act as reservoirs for electrolyte. Recently, an attractive investigation about a new class of CNC layers is proposed by Montazami and Liu *et.al* by adopting the LbL self-assembly technique[9-12]. They demonstrated that a uniform porous CNC layer can be formed by adopting spherical AuNPs and PAH, and a better electromechanical behavior of the IPMC actuators can be achieved.

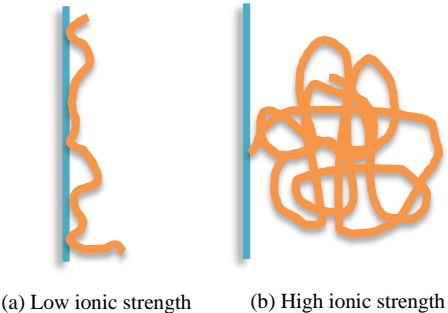


**Fig. 3.1 Schematic representation of the effects of salt concentration in the solvent environment on the conformation of polyelectrolyte; (a) low ionic strength (low salt concentration); (b) high ionic strength (high salt concentration).**

LbL self-assembly technique presents a new approach to the formation of supramolecular architectures, and many experimental results demonstrate that several factors during the fabrication process have a significant effect on the final three-dimensional multilayered structures. In the early papers from 1997, Hammond *et.al* have focused on the work about LbL adsorption of a strong polycation and polyanion and presented the effects of molecular weight[13] and ion type[14] on the adsorption process and final morphology of the obtained thin-film. Some interesting behaviors generated by the alternate assembly multilayers of polyelectrolytes and nanoparticles and corresponding influences of conditions, polyelectrolytes and nanoparticles characteristics have also been discussed[15–18]. In these papers, an important influence factor that has been pointed out is the effect of the presence of salt ions on the selectivity of deposition and the final three-dimension structure of the thin-film[19–21]. The LbL assembly process is the technique based on the ionic forces between two polyelectrolytes (or nanoparticles) to form the uniform and thin films. Therefore, the presence of salt ions will significantly affect the conformation of adsorbed polyelectrolytes and shield the charges on the repeat units. Typically, during the polyelectrolyte adsorption, the polymer chain behaviors in a more open and loose form due to the electrostatic force exerted by the

charges presented to the backbone if low salt concentration in its solvent environment, as shown in Fig. 3.1 (a); however, while the salt concentration becomes high enough to screen the charge repulsion, the polyelectrolyte will begin to minimize the interaction with the solvent, which will lead to a more compacted and dense thin-film structure, as shown in Fig. 3.1 (b).

Our working hypothesis in this work is that when we choose LbL self-assembly technique for the CNC layer fabrication, the change of salt concentration in polyelectrolyte will influence both thickness and structure of CNC layer. These changes, as well as the charge density on each of the two regions, will indicate the actuation and sensing performance of IPMC transducers. As discussed below, we choose NaCl to control the ionic strength by changing its concentration in PAH solution. We expect that the addition of NaCl can provide a better thickness and structure of CNC layers for the performance of IPMC transducers. Experimental results prove that a higher ionic strength during the LbL deposition leads to a thicker and more compacted CNC film and facilitates a more uniform distribution of AuNPs. Also, the scatter of mobile ions ( $\text{Na}^+$  and  $\text{Cl}^-$ ) in CNC can effectively screen the repulsive force by ions of the same charges that have already moved into the CNC at any given time.

### **3.2 Experimental section**

Two groups of IPMC transducers are prepared in this work. In group 1, a set of IPMC transducers with different number of bilayers (0, 10, 20, 30 and 40) were prepared with the same fabrication process as shown in section 2.2.1. In group 2, we adopted the same fabrication process except that 200 mM sodium chloride (NaCl, Sigma) was added into PAH solution before LbL deposition to determine the ionic effects on the CNC layers

conformation, and on the actuation and sensing performance. Characterization methods adopted for both groups were the same as shown in section 2.2.2. One more group with the addition of 20 mM NaCl in PAH was also made for UV-Vis absorbance spectrum characterization.

### 3.3 Results and discussion

#### 3.3.1 Ionic strength effect on CNC layer formation

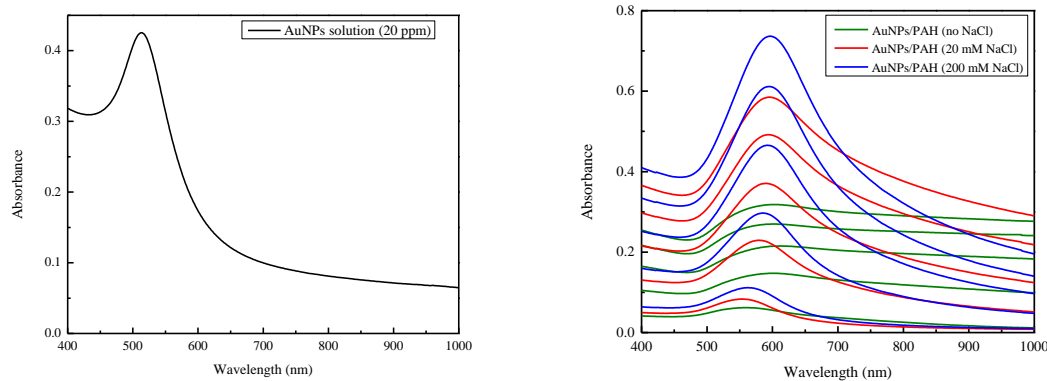


**Fig. 3.2** UV-Vis absorbance spectra of (a) AuNPs solution (20 ppm); (b) growing process of AuNPs/PAH thin-film with different salt concentrations in PAH solution. The lines from the bottom up in each color represent 2, 4, 6, 8, 10 bilayers of AuNPs/PAH thin-film respectively.

The CNC layers formation process with different contents of NaCl in PAH was characterized by UV-Vis spectroscopy, which provides a directly reception on the difference of two groups on CNC layer formation process. Fig. 3.2(a) is the UV-Vis spectrum of AuNPs solution with 20 ppm concentration (the AuNPs solution used for deposition). The distinct plasmon absorption band centered at 514 nm, corresponding to a diameter around 3 nm. In Fig. 3.2(b), the green, red and blue lines correspond to 0, 20 and 200 mM NaCl in PAH solution respectively. The lines from the bottom up in each color represent 2, 4, 6, 8 and 10 bilayers of AuNPs/PAH thin-film. It is obvious to see that with the increased salt concentration, a more intensive absorption band can be achieved.

As a polycation with high charge density, PAH has a more coiling chain when in a higher salt concentration environment due to its increased screen ability. A thicker adsorbed bilayer will be obtained due to the expected expanded molecular shape. Moreover, when a polyelectrolyte (or nanoparticle) with low charge density is adsorbed, more molecular chains (or nanoparticles) are needed to reverse the surface charge to build a new foundation for the next layer adsorption. Therefore, in this case, the added salt ions shield part of the charges of both PAH and AuNPs, which increases the quantity of polymer chains or nanoparticles required for reversing the surface charge led by the pre-deposited layer[22]. Both PAH and AuNPs layers become thicker, and the increased thickness of AuNPs layer has been demonstrated by the UV-Vis spectra shown in Fig. 3.2(b). The other important point to notice is that for the CNC formation process without any salt ions added (represented by green lines), there is a shift toward higher wavelength of the absorption band (from 514 nm to 600 nm) and the band becomes broader with the increased number of bilayers. It is believed to be the strong electromagnetic coupling between neighboring nanoparticles[23]. However, with the increased salt content in PAH solution, this phenomenon becomes less and less distinct, as shown in red and blue lines. We speculate it is because of the permeation and existence of salt ions ( $\text{Na}^+$  and  $\text{Cl}^-$ ) in the multilayers that effectively inhibits the aggregation of nanoparticles during the deposition and shields part of the electromagnetic coupling between neighboring particles, which indicates a more homogeneous distribution of AuNPs among the CNC layer.

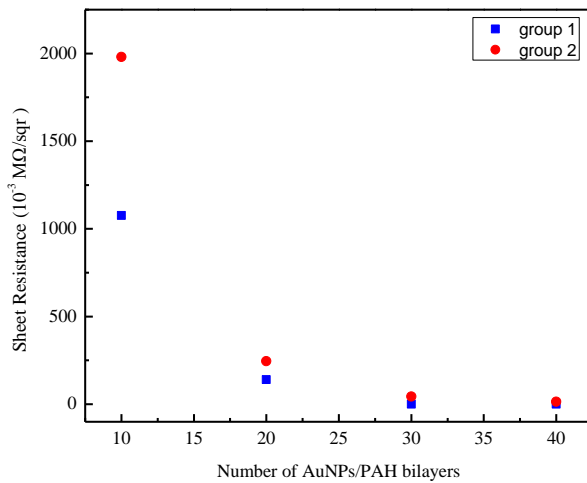


**Fig. 3.3 Difference of sheet resistance between group 1 and 2. For both groups, sheet resistance decreases significantly as the number of AuNPs/PAH bilayers increased.**

Consider the unique geometry of CNC layer, while its thickness is much smaller than its planar area, four-point-probe method was used to measure the sheet resistance of samples in two groups and the result was shown in Fig. 3.3. As expected, for each group, the sheet resistance decreases significantly as number of bilayers of AuNPs/PAH increased from 10 to 40. While the existence of PAH does not have too much attribution to the electrical conductivity of CNC, the increasing conductivity is due to a higher concentration and a higher interconnectivity of the conductive gold nanoparticles while the number of AuNPs/PAH bilayers increases. Another important point to notice is that for each 10 bilayers from 10 to 40, the sheet resistance of group 2 is always larger than that of group 1, especially in the lower bilayers range. UV-Vis spectra shown in Fig. 3.2(b) confirm the fact that the AuNPs layer becomes thicker with the increased ionic strength, thus the reasonable explanation for the increased sheet resistance may be a larger amount of PAH chains adsorbed due to the presence of salt ions when compared with the increased amount of AuNPs. That is, the increased electrical conductivity by the

added amount of AuNPs may be offset even overtaken by PAH which increases at a higher rate.

As talked in the previous chapter, we believe that a better electrically conductive structure is preferred since it can promote the motion of ions through CNC layer when an electrical field is applied. However, we also believe that there are three other factors beneficial to the performance of IPMC transducer will be improved significantly. First, as shown in the paper by Montazami *et.al*, a thicker CNC layer is capable of containing more electrolytes and hence generates a larger volume imbalance between the electrodes; as a result, a larger mechanical deformation will be obtained[10]. In this work, with the existence of salt ions, a thicker bilayer will be achieved due to (a) the polymer chains change in the shape and conformation, and (b) larger amounts of polymer chains and nanoparticles required in each layer adsorption. Second, the UV-Vis spectra in Fig. 3.2(b) indicate a more uniform distribution of AuNPs in CNC due to the shielding of part of the electromagnetic coupling between neighboring particles by the presence of  $\text{Na}^+$  and  $\text{Cl}^-$ . The porosity of the CNC allows ions to easily move through the nanostructure and then accumulate at the electrodes, leading a larger deformation if applied a voltage or generating a larger signal if applied a mechanical deformation. The more uniform distribution of AuNPs provides a more homogeneous nanostructure and a more uniform distribution of gold-ion interfacial area, promoting the motion of ions in the nanostructure and accumulation at the electrode. The last but not the least, the dispersion of salt ions ( $\text{Na}^+$  and  $\text{Cl}^-$ ) among CNC plays an important role in the screening of the repulsive force from the ions with same charge that have already moved into the CNC. Later experimental results proved that although the conductivity decreases with salt ions

addition, both actuator and sensor functions of IPMC have been improved, indicating the important attribution of the above three factors. More details will be discussed later.

### 3.3.2 Ionic strength effect on actuation performance in IPMC

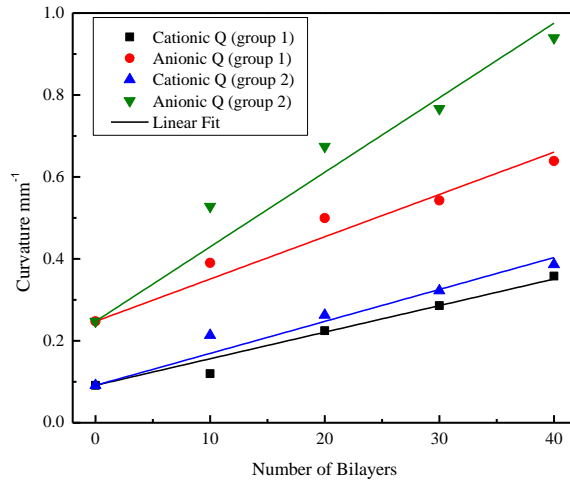


**Fig. 3.4 Cationic and anionic bending curvatures (Q) of group 1 and 2; for each group, Q increases linearly with the increased number of bilayers. Both cationic and anionic curvatures in group 2 are higher than those in group 1.**

**Table 3.1 Intercepts and slopes of the fitted lines of cationic and anionic curvatures for group 1 and 2.**

	Cationic Q (mm <sup>-1</sup> ) group 1	Cationic Q (mm <sup>-1</sup> ) group 2	Anionic Q (mm <sup>-1</sup> ) group 1	Anionic Q (mm <sup>-1</sup> ) group 2
<b>Intercept (mm<sup>-1</sup>/bilayer)</b>	0.09139	0.09139	0.24757	0.24757
<b>Slope (mm<sup>-1</sup>)</b>	0.00648	0.0078	0.01032	0.01819

IPMC actuator with ionic liquid EMI-Tf supplying the mobile ions first exhibits a fast and small bending toward to the anode led by the quick motion of  $\text{EMI}^+$  cations; then this quick and small cationic strain is cancelled by another slow and effective bending strain toward the cathode led by the moving  $\text{Tf}^-$  anions or anionic complexes(e.g.  $\text{Tf}^- \text{EMI}^+ \text{-Tf}$ )[9, 24]. As shown in Fig. 3.4, for each group, both cationic and anionic

curvatures are increased linearly with the increased number of bilayers and the slopes and intercepts of four fitted lines are represented in Table. 3.1. When comparing the cationic curvatures between group 1 and group 2, the slope increased from  $0.00648 \text{ mm}^{-1}/\text{bilayer}$  to  $0.0078 \text{ mm}^{-1}/\text{bilayer}$  with the same intercept  $0.09139 \text{ mm}^{-1}$  after the addition of salt ions, indicating a higher growth trend and a higher curvature at each number of bilayers. Since bending time due to cationic motion is limited because of the subsequent anionic motion to the opposite direction, the larger cationic curvature corresponds to a quicker motion of  $\text{EMI}^+$  cations through CNC. Consider the result in Fig. 3.3 that the electrical conductivity has a little decrease after the addition of salt ions, a reasonable explanation of this phenomenon is that the dispersion of ions in the CNC can effectively screen the repulsive force from the ions with same charge that have already moved into the CNC. Meanwhile, the more homogeneous distribution of AuNPs among CNC may also play a role in increasing the motion of ions. The anionic curvature slope after salt ions addition is from  $0.01032 \text{ mm}^{-1}/\text{bilayer}$  to  $0.01819 \text{ mm}^{-1}/\text{bilayer}$  with the same intercept at 0 bilayer ( $0.24757 \text{ mm}^{-1}$ ). Besides the screen impact of salt ions as we talked above, a more important reason is the attribution of the thicker CNC layer, which is capable to contain a larger amount of ions and hence generate a larger volume imbalance between two electrodes[10].

### **3.3.3 Ionic strength effect on sensing performance in IPMC**

Basically, when IPMC is bent or applied a mechanical deformation, some of the solvent carrying charged ions will prefer to shift to their favored region where opposite charges are available. This in turn generates an electric field and the associated voltage[25]. While the principle of sensing is the reverse of actuation, we believe that the

changes of structure and thickness of CNC due to the addition of the salt ions also have an important influence on the sensor function of IPMC. Two samples with 40 bilayers from group 1 and 2 respectively were used for the sensing test in this part, and the sample with bare Nafion membrane (0 bilayer) was also adopted for comparison. For the quasi-static sensing test, the samples were covered between two electrical tapes with copper as electrode connecting to a digital phosphor oscilloscope to record the generated voltage. The voltages of three samples are represented in Fig. 3.5 and the experimental result indicates that when same mechanical bending is applied, the sample from group 2 (rightmost) outputs the largest electrical signal when compared with the other two. As proved before, we believe it is attributed by the change of CNC layer's thickness and structure due to the changes in the chain conformation and molecular shape. In this case, a thicker layer will be obtained and previous experimental results showed that a thicker CNC layer is beneficial for both IPMC actuator and sensor functions.

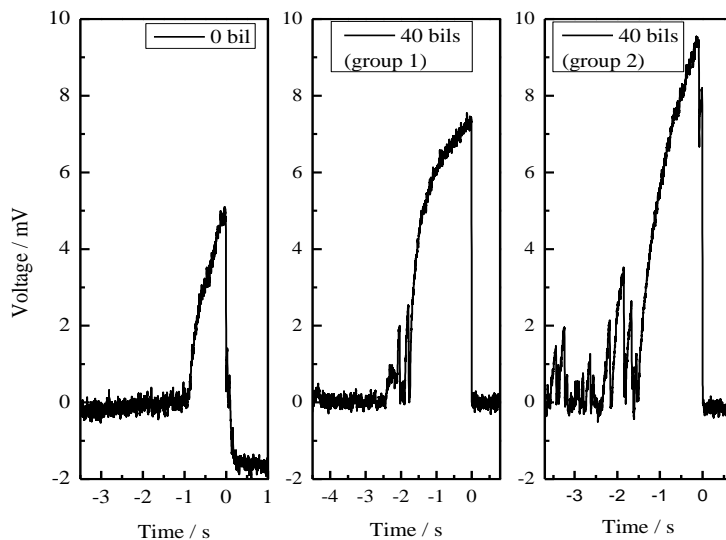


**Fig. 3.5 IPMC sensor response in the form of output voltage when IPMC sensor is subject to a bending deformation. From left to right is the voltage generated by the sample with bare Nafion membrane (0 bilayer), 40 bilayers from group 1 and 40 bilayers from group 2.**

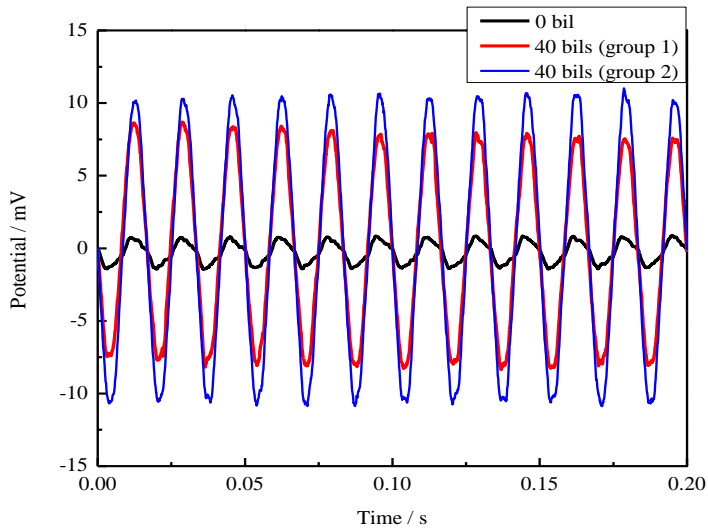


**Fig. 3.6 IPMC sensor response in the form of output voltage when IPMC sensor is subject to a dynamic vibration impact by a motor. Black line is corresponding to the sample with bare Nafion membrane (0 bilayer), red and blue lines are corresponding to the samples with 40 bilayers from group 1 and 2 respectively.**

Meanwhile, as the result shown in Fig. 3.6, when the strips of IPMC sensor are dynamically distributed by a dynamic impact led by a motor with constant vibration frequency, the existence of salt ions also provides a significant enhancement on the amplitude of the generated voltage while does not damp the signal's frequency. It indicates a higher moving speed of the ions through CNC. Consider the low electrical conductivity of the CNC of group 2 when compared with group 1, we conclude it is due to the dispersion of salt ions ( $\text{Na}^+$  and  $\text{Cl}^-$ ) which can effectively screen the repulsive force from the ions with the same charge that have already moved into CNC. This phenomenon is also keeping consistent in the analysis we made in section 3.3.2.

### 3.4 Conclusion

We have adopted LbL self-assembly technique for the fabrication of CNC nanostructure in IPMC transducers. Some published papers demonstrate that the addition

of small salt molecule (NaCl in this work) can increase the ionic strength of the polyelectrolyte solution and then change the polymer chains conformation and molecular shape, which leads to a higher thickness and a different structure of CNC. After the addition of NaCl in PAH, the generated CNC has a higher thickness and a more homogenous distribution of AuNPs which has been confirmed by the UV-Vis spectra; it still demonstrates a lower electrical conductivity which is proved by the sheet resistance measurement. Consider the little attribution to the electrical conductivity by PAH, one reasonable explanation is that the increased electrical conductivity by the added amount of AuNPs may be offset even overtaken by PAH which increases at a higher rate. The influence of the addition salt ions on the actuator and sensor functions of IPMC has also been studied in this work. With the improved ionic strength, the cationic curvature increased linearly with the increased number of bilayers at the rate of  $0.0078 \text{ mm}^{-1}/\text{bilayer}$ , larger than the increasing rate of samples before the addition of salt ( $0.00648 \text{ mm}^{-1}/\text{bilayer}$ ). This phenomenon indicates a quicker motion of  $\text{EMI}^+$  cations through CNC. It may be led by the dispersion of salt ions ( $\text{Na}^+$  and  $\text{Cl}^-$ ) which is beneficial for screening the repulsive force from the ions with same charges that have already moved in CNC. Meanwhile, the slope of fitted line of anionic curvature increased from  $0.01032 \text{ mm}^{-1}/\text{bilayer}$  to  $0.01819 \text{ mm}^{-1}/\text{bilayer}$  after the ionic strength was improved. An important reason of this phenomenon is the capacity of containing larger amount of polyelectrolyte of a thicker CNC as well as the screen role of the existence of salt ions. Sensor function measurement indicates that with the enhanced ionic strength, the generated voltage has also been improved significantly when apply IPMC sensor to quasi-static or dynamic impact loading. The improved actuator and sensor functions

achieved in this work demonstrate a positive influence of ionic strength on CNC structure and on the performance of IPMC transducers.

## Reference

- [1] M. Shahinpoor and K. J. Kim, “Ionic polymer–metal composites: III. Modeling and simulation as biomimetic sensors, actuators, transducers, and artificial muscles,” *Smart Materials and Structures*, vol. 13, no. 6, pp. 1362–1388, Dec. 2004.
- [2] M. Shahinpoor and K. J. Kim, “Ionic polymer–metal composites: IV. Industrial and medical applications,” *Smart Materials and Structures*, vol. 14, no. 1, pp. 197–214, Feb. 2005.
- [3] K. J. Kim and M. Shahinpoor, “Ionic polymer metal composites: II. Manufacturing techniques,” *Smart Materials and Structures*, vol. 12, no. 1, pp. 65–79, Feb. 2003.
- [4] M. Shahinpoor and K. Kim, “Ionic polymer-metal composites: I. Fundamentals,” *Smart Materials and Structures*, vol. 10, pp. 819–833, 2001.
- [5] D. Pugal, K. Jung, A. Aabloo, and K. J. Kim, “Ionic polymer-metal composite mechanoelectrical transduction: review and perspectives,” *Polymer International*, vol. 59, no. 3, pp. 279–289, Jan. 2010.
- [6] M. Shahinpoor, “Ionic polymer-metal composites (IPMCs) as biomimetic sensors, actuators and artificial muscles-a review,” *Smart Materials and Structures*, vol. 7, no. 6, pp. R15–R30, 1998.
- [7] B. Kim, D.-H. Kim, J. Jung, and J.-O. Park, “A biomimetic undulatory tadpole robot using ionic polymer–metal composite actuators,” *Smart Materials and Structures*, vol. 14, no. 6, pp. 1579–1585, Dec. 2005.
- [8] C. Bonomo, P. Brunetto, L. Fortuna, P. Giannone, S. Graziani, and S. Strazzeri, “A Tactile Sensor for Biomedical Applications Based on IPMCs,” *IEEE Sensors Journal*, vol. 8, no. 8, pp. 1486–1493, Aug. 2008.
- [9] R. Montazami, D. Wang, and J. Heflin, “Influence of conductive network composite structure on the electromechanical performance of ionic electroactive polymer actuators,” *International Journal of Smart and Nano Materials*, vol. 3, no. 3, pp. 204–213, Sep. 2012.
- [10] R. Montazami, S. Liu, Y. Liu, D. Wang, Q. Zhang, and J. R. Heflin, “Thickness dependence of curvature, strain, and response time in ionic electroactive polymer actuators fabricated via layer-by-layer assembly,” *Journal of Applied Physics*, vol. 109, no. 10, pp. 104301, 2011.
- [11] S. Liu, R. Montazami, Y. Liu, V. Jain, M. Lin, X. Zhou, J. R. Heflin, and Q. M. Zhang, “Influence of the conductor network composites on the electromechanical performance of ionic polymer conductor network composite actuators,” *Sensors and Actuators A: Physical*, vol. 157, no. 2, pp. 267–275, Feb. 2010.
- [12] S. Liu, R. Montazami, Y. Liu, V. Jain, M. Lin, J. R. Heflin, and Q. M. Zhang, “Layer-by-layer self-assembled conductor network composites in ionic polymer metal composite actuators with high strain response,” *Applied Physics Letters*, vol. 95, no. 2, pp. 023505, 2009.
- [13] S. L. Clark, M. Montague, and P. T. Hammond, “Selective deposition in multilayer assembly: SAMs as molecular templates,” *Supramolecular Science*, vol. 4, no. 1–2, pp. 141–146, Mar. 1997.

- [14] S. Clark, M. Montague, and P. Hammond, "The effect of ion type and ionic content on templating patterned ionic multilayers," *ACS Symposium Series*, vol. 695, pp. 206–219, 1998.
- [15] G. Bogdanovic, T. Sennerfors, B. Zhmud, and F. Tiberg, "Formation and Structure of Polyelectrolyte and Nanoparticle Multilayers: Effect of Particle Characteristics," *Journal of Colloid and Interface Science*, vol. 255, no. 1, pp. 44–51, Nov. 2002.
- [16] Y. Lvov, K. Ariga, M. Onda, I. Ichinose, and T. Kunitake, "Alternate assembly of ordered multilayers of SiO<sub>2</sub> and other nanoparticles and polyions," *Langmuir*, vol. 13, no. 23, pp. 6195–6203, 1997.
- [17] A. Kampes and B. Tieke, "Self-assembly of carboxylated latex particles at charged surfaces: influences of preparation conditions on the state of order of the monolayers," *Materials Science and Engineering: C*, vol. 8–9, pp. 195–204, Dec. 1999.
- [18] T. Serizawa, H. Takeshita, and M. Akashi, "Electrostatic adsorption of polystyrene nanospheres onto the surface of an ultrathin polymer film prepared by using an alternate adsorption technique," *Langmuir*, vol. 14, no. 15, pp. 4088–4094, 1998.
- [19] Y. Lvov, G. Decher, and H. Moehwald, "Assembly, structural characterization, and thermal behavior of layer-by-layer deposited ultrathin films of poly (vinyl sulfate) and poly (allylamine)," *Langmuir*, vol. 9, no. 2, pp. 481–486, 1993.
- [20] S. Clark, M. Montague, and P. Hammond, "Ionic effects of sodium chloride on the templated deposition of polyelectrolytes using layer-by-layer ionic assembly," *Macromolecules*, vol. 30, no. 23, pp. 7237–7244, 1997.
- [21] S. Ghannoum, Y. Xin, J. Jaber, and L. Halaoui, "Self-assembly of polyacrylate-capped platinum nanoparticles on a polyelectrolyte surface: Kinetics of adsorption and effect of ionic strength and deposition protocol," *Langmuir*, vol. 19, no. 11, pp. 4804–4811, 2003.
- [22] Q. Sun, Z. Tong, C. Wang, B. Ren, X. Liu, and F. Zeng, "Charge density threshold for LbL self-assembly and small molecule diffusion in polyelectrolyte multilayer films," *Polymer*, vol. 46, no. 13, pp. 4958–4966, Jun. 2005.
- [23] X. Hu, W. Cheng, T. Wang, Y. Wang, E. Wang, and S. Dong, "Fabrication, characterization, and application in SERS of self-assembled polyelectrolyte-gold nanorod multilayered films," *The journal of physical chemistry. B*, vol. 109, no. 41, pp. 19385–9, Oct. 2005.
- [24] J. Hou, Z. Zhang, and L. a Madsen, "Cation/anion associations in ionic liquids modulated by hydration and ionic medium," *The journal of physical chemistry. B*, vol. 115, no. 16, pp. 4576–82, Apr. 2011.
- [25] M. Shahinpoor, "Ionic polymer-metal composites (IPMCs) as biomimetic sensors, actuators and artificial muscles-a review," *Smart Materials and Structures*, vol. 7, no. 6, pp. R15–R30, 1998.

## CHAPTER 4

### Future Prospective

#### **4.1 Exploration of cytotoxicity of IPMC transducer**

In conclusion, ionic polymer-metal composite (IPMC) transducers with two layers of conductive network composite (CNC) fabricated by layer by layer (LbL) controlled self-assembly technique have unique structural properties, which makes them suitable for wide range of potential applications as soft robotic actuators, dynamic sensors and artificial muscles in the areas of aerospace, mechanical engineering and even biological and biomedical engineering. However, when exposed to bioenvironments, nanoparticles, one important component of CNC layers in IMPC transducer, exhibit different and potentially hazardous chemical and electrochemical properties, when compared with bulk material. While efforts in colloid and polymer science are mainly focused on phase diagrams and mechanisms of nanoparticle stability and synthesis, little fundamental work appears about molecular mechanisms of health hazards and cytotoxicity of nanoparticles. This presents a problem when IPMC transducers are introduced to bioenvironments for biological applications. Since the nanomaterials exposed to bioenvironments may participate and even interfere with biochemical reactions; oxidation and oxidative stress are among the risks posed to the cellular and sub-cellular environment. These redox properties may not be directly measurable within a bioenvironment, but can be quantified through well-defined electrochemical reactions. Therefore, a well-defined electrochemical measurement method to measure and quantify redox properties of different kinds of nanoparticles seems to be necessary in the future works.

Electrochemical methods, when combined with complementary techniques, such as

optical spectroscopy, offer unique approaches to investigate and understand structure-property-toxicity relationships. Traditional approach to study the redox chemistry of nanoparticles would be to treat them as dissolved analytes, yet this method would lead to solution degradation due to the presence of an electric field and thus disturbance of functional groups on the nanoparticles. Considering the specific constitution form of nanoparticles in IPMC transducer, we have adopted LbL controlled self-assembly technique to fabricate well-defined nanoparticle-polyelectrolyte complexes at the electrode that eliminate these drawbacks.

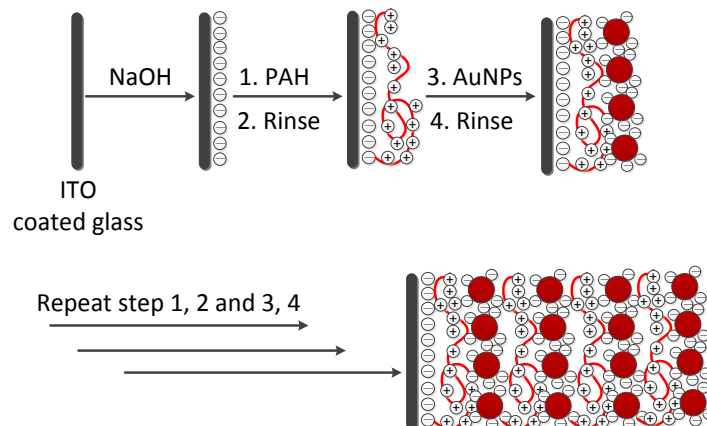


**Fig. 4.1 Formation of AuNPs/PAH thin-film via LbL process.**

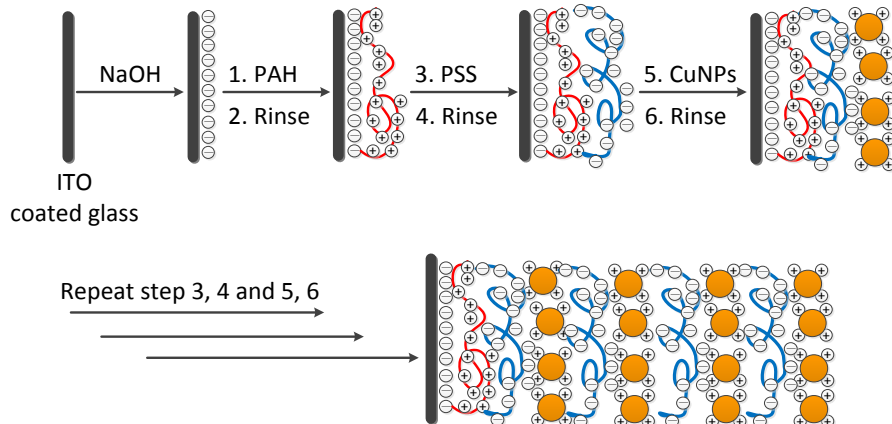


**Fig. 4.2 Formation of CuNPs/PSS thin-film via LbL Process.**

In our current work, gold nanoparticles (AuNPs) (diameter ~3 nm, 99.99%, 20 ppm aqueous) and copper nanoparticles (CuNPs) (diameter~20nm, 99.99%, 20 ppm aqueous) were used to start initial exploration. Poly-(allylamine hydrochloride) (PAH) and poly(sodium styrenesulfonate) (PSS) were used as partner polyelectrolytes for AuNPs and CuNPs respectively; indium tin oxide (ITO) coated glass was used as substrate. Presented in Fig. 4.1 and 4.2 are the LbL self-assembly deposition process of AuNPs/PAH and CuNPs/PSS thin-films.

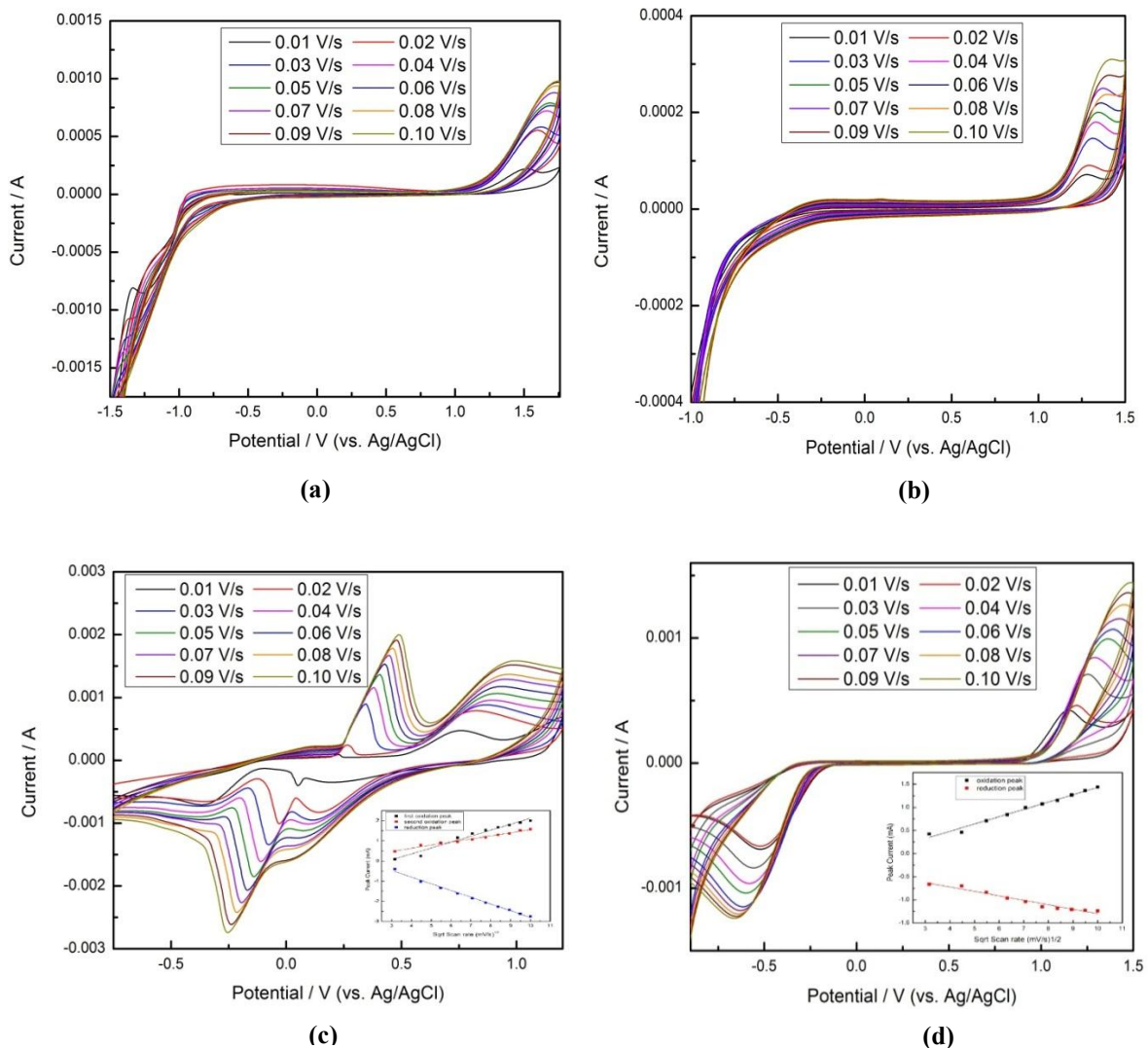


**Fig. 4.3** Cyclic voltammograms of (a) bare ITO coated glass, (b) PAH/PSS thin-film, (c) AuNPs/PAH thin-film, and (d) CuNPs/PSS thin-film taken at 10-100 mV/s scan rates (10 mV/s increments). Inset in (c) and (d) : peak current vs. square root of scan rate indicates diffusion controlled process.

The redox properties of AuNPs/PAH and CuNPs/PSS thin-films were investigated using cyclic voltammetry (CV). The scanning ranges were relative large to include most redox peaks at different scan rates, and the results are shown in Fig. 4.3(c) and 4.3(d). Fig. 4.3(a) and 4.3(b) represent the cyclic voltammograms of bare ITO coated glass and PAH/PSS thin-film respectively for comparison.

When compared with cyclic voltammograms of bare ITO coated glass, AuNPs/PAH thin-film shows two more pairs of redox peaks. One is related to the redox process of AuNPs and the other one is related to the redox process of the functional group on AuNPs surface. CuNPs/PSS thin-film shows an oxidation peak at the same position with PAH/PSS thin-film but with a much higher strength, indicating that the oxidation reaction of both CuNPs and PSS may appear at the approximately same voltage. The new reduction peak in the reductive scan may be related to the reduction reaction of CuNPs. The hysteresis between oxidation and reduction peaks in both AuNPs/PAH and CuNPs/PSS films was increased with increasing scan rate, due to either slow electron transfer between ITO and nanoparticle/polyelectrolyte thin-films, or the internal resistance of the bulk of the films[1]. All oxidation and reduction peak current rise linearly with the square root of the scan rate, indicating a primarily diffusion controlled electrochemical reaction.

It was also observed that different ionic strengths during the LBL self-assembly process to some extent control the redox properties of nanoparticle-partner polyelectrolyte complexes. As discussed in Chapter 3, the ions will screen the charges attached to the chains when the polyelectrolyte is dissolved in the solvent. While the

charges presented on the polymer backbone are the dominant force controlling conformation, it will exert an electrostatic force that drives the polymer into a more open and loose conformation. However, if certain concentration of salt exists in the surrounding solution, this charge repulsion will be screened and the polyelectrolyte will begin to minimize the interaction with the solvent, which will lead to a more compacted and dense thin-film structure after the LBL self-assembly deposition. Results represented in Chapter 3 (Fig. 3.2(b), 3.3-3.6) show a difference in the thin-film thickness and structure after the addition of NaCl in PAH before LbL deposition, which have a significant effect on the actuation and sensing behavior of IPMC transducers. Therefore, we speculate that the ionic strength of polyelectrolyte solution also has influence on the redox properties of nanoparticles-polyelectrolyte complexes and has potential effect on their cytotoxicity when exposed to bioenvironments.

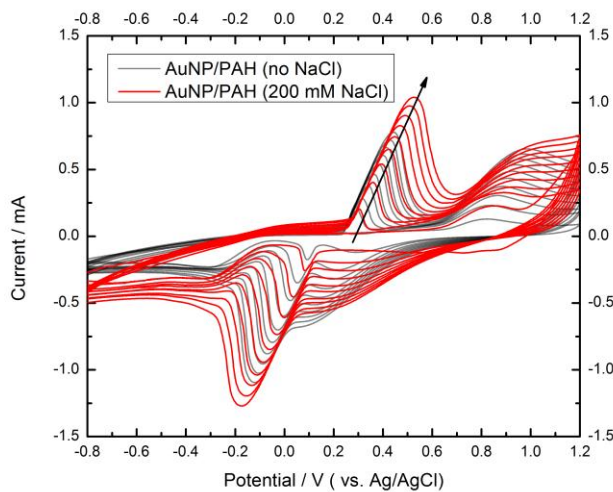


**Fig. 4.4** Cyclic voltammograms of AuNPs/PAH thin-film taken at 10-100 mV/s scan rates (10 mV/s increments). Black lines represent CV result of thin-film with no NaCl in PAH solution while the red lines represent CV result of thin-film with 200 mM NaCl in PAH solution. Arrow indicates increasing scan rate.

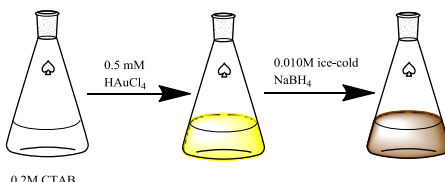
The redox properties of AuNPs/PAH complexes with different ionic strength (0 and 200 mM NaCl in PAH solution) have been measured by CV and the corresponding comparison result is shown in Fig. 4.4. It can be found that the peak strength has increased and the distance between the redox peaks has become wider with the addition of NaCl in PAH solution. The increased hysteresis between oxidation and reduction peaks confirms a more compacted and dense structure of the AuNPs/PAH thin-film which will lead to a higher internal resistance of the bulk of the film.

Exploration on the cytotoxicity of IPMC actuators and sensors provides a theoretical foundation for their further applications especially when implanted into bioenvironment. Some related work is in progress and the results have been shown above. To have a much deeper understanding, a more completed and comprehensive research is needed in the future.

#### **4.2 Exploration of effect of nanoparticles size and shape on IPMC transducer performance**

Experimental results indicated that porous electrodes is preferred to improve the IMPC transducer performance since it can provide higher contact areas between electrodes and ionic polymers so that a higher population of excess charges will be obtained at the electrodes. Therefore two conductive network composite (CNC) layers were used to improve the porosity of electrodes. We have adopted LbL technique to get a porous CNC layer structure based on AuNPs/PAH thin-film, which provides a significant improvement on the actuation and sensing performance. Moreover, we believe that different shape and size of nanoparticles also have a significant effect on the CNC layer structures and thus the performance of IPMC transducers.

## Seed solution preparation



## Growth of AuNRs with seed solution

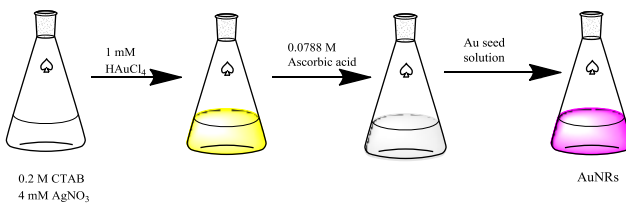


**Fig. 4.5 Synthesis process of AuNRs via seed mediated method.**

In 2003, Nikoobakht *et.al* has used seed-mediated growth method for preparing gold nanorods (AuNRs) with aspect ratios ranging from 1.5 to 10[2]. Briefly, hexadecyltrimethyl ammonium bromide (CTAB)-capped AuNPs were synthesized by chemical reduction of gold (III) chloride hydrate ( $\text{HAuCl}_4 \cdot x\text{H}_2\text{O}$ ) with sodium borohydride ( $\text{NaBH}_4$ ) as seed at first. Then the seed was added to the growth solution for the rodlike particles growth with more  $\text{HAuCl}_4$  as gold supply, silver nitrate ( $\text{AgNO}_3$ ) and L-ascorbic acid as weak reducing agent, and CTAB as surfactant. Different aspect ratios can be achieved by controlling Ag ion concentration in the growth solution. A schematic representation of AuNRs synthesis process is shown in Fig. 4.5. The first line represents the seed solution preparation, where the brownish yellow solution in the third flask indicates the formation of gold seeds used for the AuNRs growing. Growth process is represented in the second line. After the addition of ascorbic acid, the  $\text{HAuCl}_4$  solution becomes colorless from light yellow since ascorbic acid acts as a mild reductant. Then certain amount of seed solution prepared in the first step is added and after keep the

mixture solution at 27-30 °C for a whole night, a wine red AuNRs solution can be achieved. Moreover, Sau *et.al* described that by systematic variation of experimental parameters in the seed-mediated growth method, a number of structural architectures of Au nanoparticles, from rod, rectangle, hexagon, cube, triangle and starlike outlines to branch, can be achieved in high yield at room temperature[3].

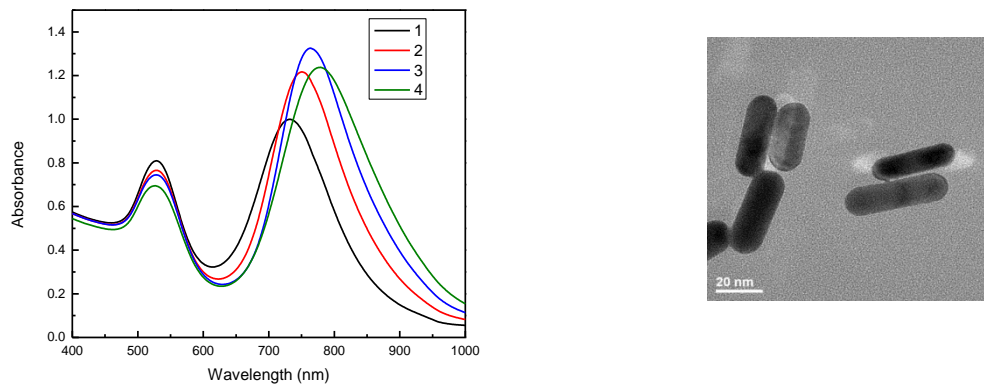


**Fig. 4.6 (a)** UV-Vis absorbance spectra of AuNRs with different Ag ion concentrations; **(b)** TEM image of AuNRs with aspect ratio around 2.3.

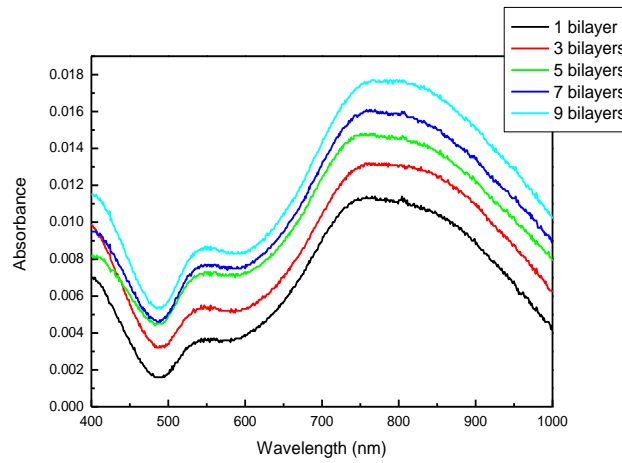


**Fig. 4.7** UV-Vis absorbance spectra of growing process of AuNRs/PSS multilayer film.

Fig. 4.6(a) is our experiment results showing the UV-Vis spectra of AuNRs with different Ag ion concentration in the growth solution (line 1, 2, 3 and 4 corresponds to

lowest, lower, higher and highest Ag ion concentration respectively) and Fig. 4.6(b) is the TEM image of AuNRs corresponding to line 1 with aspect ratio around 2.3 . The first absorption band around 530 nm is assigned to the traverse plasmon resonance band of AuNRs, and the other absorption band located on a longer wavelength (700-850 nm) corresponds to the longitudinal plasmon resonance band of AuNRs. With the redshift of the longitudinal plasmon resonance band, the aspect ratio of AuNRs has increased with an increasing silver concentration. Moreover, consider the positive surface charge of AuNRs (led by the CTAB double-layer cover), PSS was used as partner polyelectrolyte with AuNRs for the formation of LbL self-assembly controlled thin-film. The formation process was measured by UV-Vis spectrometry and the result is represented in Fig. 4.7. Based on these experiment results we have obtained, exploring the effect of size and shape of nanoparticles on the CNC layers structure and on the IPMC transducers performance is optimistic and meaningful in our next step.

## Reference

- [1] R. Montazami, V. Jain, and J. R. Heflin, "High contrast asymmetric solid state electrochromic devices based on layer-by-layer deposition of polyaniline and poly(aniline sulfonic acid)," *Electrochimica Acta*, vol. 56, no. 2, pp. 990–994, Dec. 2010.
- [2] B. Nikoobakht and M. El-Sayed, "Preparation and growth mechanism of gold nanorods (NRs) using seed-mediated growth method," *Chemistry of Materials*, vol. 15, no. 10, pp. 1957–1962, 2003.
- [3] T. K. Sau and C. J. Murphy, "Room temperature, high-yield synthesis of multiple shapes of gold nanoparticles in aqueous solution," *Journal of the American Chemical Society*, vol. 126, no. 28, pp. 8648–8649, Jul. 2004.

## Acknowledgement

My deepest gratitude goes first and foremost to Dr. Reza Montazami, my major professor, for his constant help, support, encouragement and guidance. He has provided sound advice and lots of good ideas on my thesis-writing period and master-study period since the time I joined his group in 2011. His astounding knowledge and enthusiastic help make work interesting for me, and I have learned and improved a lot during the past two years. Without his consistent and illuminating instruction, this thesis could not have reached its present form.

Secondly, I should give my hearty thanks to Dr. Michael Kessler and Dr. Xinwei Wang as my thesis committee members. Their patient instructions and precious suggestions help me a lot for my study and work.

I would also like to thank my labmates, Dr. Handan Acar and Ruisi Zhang for the helpful discussions, latest literature sharing and all the fun we had in the lab.

Last my thanks would go to my beloved family. I would thank my parents for their unconditional love for me and great confidence in me all through these years. My husband Chuan Jiang is the person who is always there with me during the hardest times in my life. I own my sincere gratitude to them for what they have done for me.